Hole-transporting hydrazones

Ramūnas Lygaitis,[ab] Vytautas Getautis[c] and Juozas Vidas Grazulevicius*[a]

Received 14th January 2008
First published as an Advance Article on the web 15th February 2008
DOI: 10.1039/b702406c

This *tutorial review* covers recent contributions in the area of hole-transporting hydrazones, which are widely used in optoelectronic devices. It is addressed to students and researchers interested in the synthesis and properties of organic electroactive materials. The thermal, charge transport and other properties of electroactive hydrazones are compared and the relationships between the molecular structures and properties are emphasized. The first part discusses the low-molar-mass hydrazones and presents examples of their synthetic routes and chemical structures. In the second part, polymeric arylaldehyde hydrazones containing hydrazone moieties as the side substituents and in the main-chain are described.

Introduction

Organic semiconductors represent a type of electroactive materials which have been widely studied during the past decades. Organic semiconductors or charge transport materials are employed in various fields such as electrophotography (photoreceptors of copying machines, laser printers and modern fax machines), displays (organic light emitting diodes), power generation (solar cells), memory devices (field effect transistors) *etc*. The first industrial scale application of organic semiconductors was xerography. Of the many technologies that led to the evolution of xerography, charge transport materials played a major role.[1] In recent years, several families of hole-transporting materials have been increasingly studied. Among modern p-type semiconductors, arylamines and arylalkanes prevail. They have been recently described in detail in several comprehensive reviews.[2] This paper gives an overview of the recent developments in the synthesis and investigation of low-molar-mass and polymeric arylaldehyde hydrazones. To our knowledge, this is the first attempt to review hydrazones as charge-transport materials in a separate review article. Hydrazones are a class of molecules that contain the –CH═N–N═ functionality. Good enough charge-transporting properties for technical applications, the simple synthesis and low cost are the advantages of arylaldehyde hydrazones against other classes of charge transport materials.

[a] *Department of Organic Technology, Kaunas University of Technology, Radvilenu plentas 19, LT50254 Kaunas, Lithuania. E-mail: juozas.grazulevicius@ktu.lt*
[b] *Institute of Physics, Savanoriu ave 231, LT02300 Vilnius, Lithuania*
[c] *Department of Organic Chemistry, Kaunas University of Technology, Radvilenu plentas 19, LT50254 Kaunas, Lithuania*

Basic definitions and experimental techniques

It is generally accepted that charge transport in organic disordered systems (polymers, molecularly doped polymers, molecular glasses) takes place by a hopping process. Charge transport in organic disordered systems is understood as a sequential redox process over molecules and is generally characterized by the following features:[3] (a) transient photocurrents are often dispersive in contrast to non-dispersive photocurrents observed for organic crystalline materials, (b) drift mobilities are lower, (c) charge transport is thermally activated, and (d) charge carrier drift mobilities are electric-field-dependent. It should be noted, however, that recent studies on amorphous molecular materials have revealed that

Ramūnas Lygaitis received his Masters and PhD in Chemistry from the Kaunas University of Technology (Lithuania) in 2002 and 2007 with Prof. J. V. Grazulevicius. During his PhD studies he joined Prof. P. Strohriegl's group at the University of Bayreuth as a participant of EUROFET research training network. Presently, he is a postdoctoral fellow at the Institute of Physics in Vilnius, Lithuania. His research interests are synthesis and characterization of organic semiconducting materials.

Vytautas Getautis studied chemical technology at Kaunas University of Technology, Lithuania. He obtained a PhD in chemistry from there in 1988. From 1989 to 2005 he worked as a senior research associate at the Department of Organic chemistry of Kaunas University of Technology. Since 2006 he has been a professor in the same Department. His research interests include the synthesis and properties of photoconductive molecular glasses and investigation of the products of the interaction of aromatic amines and heterocyclic compounds with epichlorohydrin.

Juozas Vidas Grazulevicius studied chemical technology at Kaunas University of Technology, Lithuania. From 1974 to 1976 he worked in industry. He obtained a PhD in chemistry at Kaunas University of Technology in 1980. He habilitated there in 1995. Since 1995 he has been a professor at the Department of Organic Technology, Kaunas University of Technology. He has spent extensive periods at Heriot-Watt University, Edinburgh, at Lancaster University (UK), at the University of Bayreuth (Germany), and at Cergy-Pontoise University (France). His research interests include the synthesis and properties of organic semiconductors and other electroactive compounds, ionic polymerization of cyclic monomers and vinyl ethers and the photophysics of organic materials.

they exhibit almost non-dispersive photocurrents and high enough charge drift mobilities (10^{-4}–10^{-2} cm^2 V^{-1} s^{-1}). Charge transport in organic solids is most often described in the framework of the Bässler disorder formalism.[4] The model, based on Monte-Carlo simulation, has shown great success in describing charge transport properties of polymers and low-molar-mass materials. According to this model, charge transport occurs by hopping through a manifold of localized states with both energy and positional disorder.

As explained in ref. 1 and 2, when voltage is applied to a thin film of organic semiconductor that is sandwiched between two electrodes, charge carriers (holes or electrons) are transported across the sample under the electric field. The main issue with charge transport is how fast the charge carriers are transported. The velocity of charge carriers is proportional to the strength of the applied electric field (eqn (1)):[1]

$$v = \mu E \tag{1}$$

where v is the velocity of charge carriers, E is the strength of electric field, and the constant μ is the drift mobility of the charge carriers. It can be interpreted as the distance over which charge carriers are transported per second under the unit electric field. It should be noted that μ is dependent upon the electric field for organic materials and greatly depends on the molecular structures and morphology of the materials.

The most widely used technique for the estimation of charge carrier drift mobility is the time-of-flight (TOF) method. Two established techniques of TOF exist, *i.e.* the technique based on transient photocurrent measurements and the xerographic technique (XTOF) based on photoinduced discharge measurements. The former is based on the measurement of the carrier transit time (t_t), namely, the time required for a sheet of charge carriers photogenerated near one of the electrodes by pulsed light irradiation to drift across the sample to the other electrode under an applied electric field.[5] The principle of the TOF technique is shown in Fig. 1.

A thin film of photoconductive material is sandwiched between a conductive substrate, for example an aluminized mylar film, and a semitransparent top electrode and connected to a voltage source and a resistor R. Because of the blocking electrodes the source voltage appears across the film. A thin sheet of charge carriers is generated near the top electrode by a short pulse of strongly absorbed light. Due to the influence of the applied field the carriers drift across the sample towards the bottom electrode. The resulting current is measured in the external circuit at the resistor R. In the double logarithmic plot of photocurrent *versus* time, the bend at the transit time t_t is clearly detectable. The effective charge carrier mobility μ is calculated from the transit time according to eqn (2):

$$\mu = \frac{d}{t_t E} \tag{2}$$

where d denotes the layer thickness and E is the electric field strength.

A schematic representation of a XTOF experiment is shown in Fig. 2.[6]

In the xerographic technique, the sample (photoconductive material) on a conducting substrate is charged by a corona discharge and then exposed to a flash of radiation with a

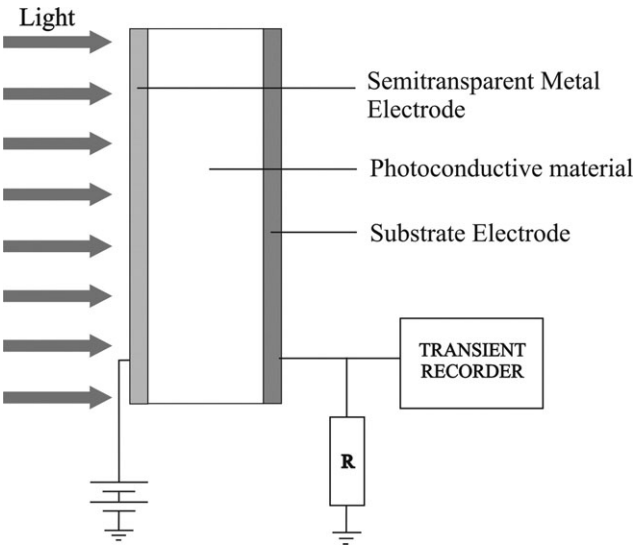

Fig. 1 Schematic representation of the transient photocurrent measurements.

duration that is short compared to the transit time. The exposure creates a sheet of carriers that are then injected into the bulk of the sample. Charge injection can be accomplished by either direct photoexcitation or from a photoemitting electrode. The measurements are usually performed under space-charge-limited conditions. As the charges drift across the sample under the action of the applied electric field, the surface potential decreases. In the double logarithmic plot of the rate of change in the surface potential *versus* time, the bend at the transit time t_t is then detected. Charge mobility (μ) is determined according eqn (3):

$$\mu = \frac{d^2}{t_t U_0} \tag{3}$$

where U_0 is the voltage applied to the sample and d is the thickness of the sample.

Two measurement modes are possible depending on the measurement circuit parameter choice, *i.e.* the current-mode and the voltage-mode. Usually dU/dt transients in the current-

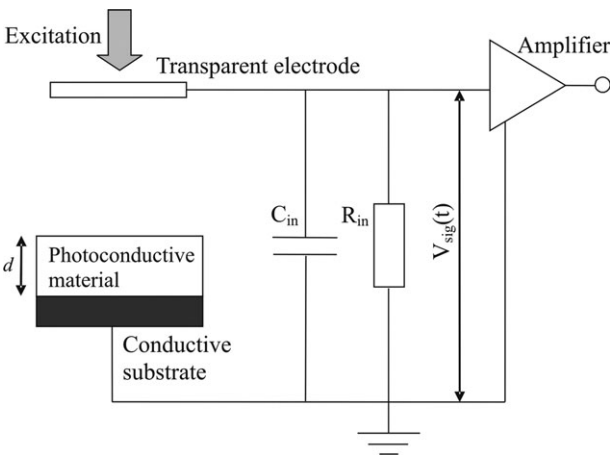

Fig. 2 Schematic representation of XTOF measurements.

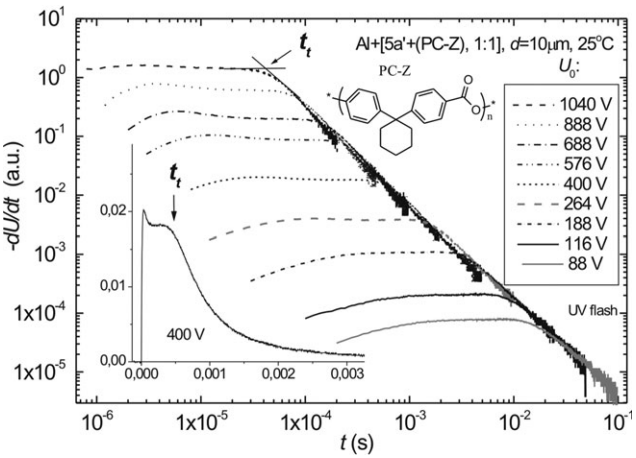

Fig. 3 Transient current waveforms for the molecular mixture of hydrazone **5a′** with bisphenol Z polycarbonate (PC-Z) for hole transport in a double logarithmic plot. The curve at $U_0 = 400$ V is plotted in the insert.

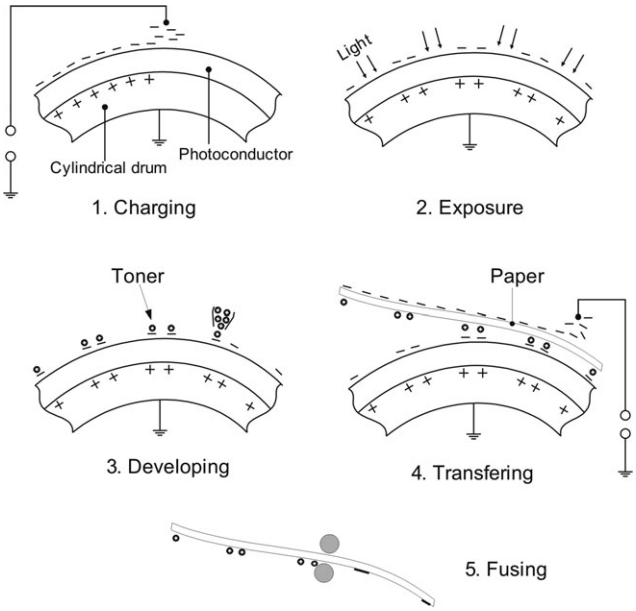

Fig. 4 Principles of the xerographic process.

mode in arbitrary units are presented. A typical experimental transit curve is shown in Fig. 3.[7]

Relative to the conventional photocurrent technique, the advantages of the photoinduced discharge TOF method are that higher fields can be sustained without dielectric breakdown and experimental simplicity.

In the design and construction of organic optoelectronic devices, energy level differences in organic semiconductors are of great importance. Two parameters that describe the highest occupied molecular orbital (HOMO) and lowest unoccupied molecular orbital (LUMO) energy levels with respect to the vacuum level correspond to the ionization potential (I_p) and the electron affinity (A), respectively.

The ionization potentials of the films of organic compounds can be established by the electron photoemission technique from the dependency of the photocurrent (I) on the incident light quanta energy, which is named as electron photoemission spectra and plotted as $I^{0.5} = f(h\nu)$. Usually the dependence of the photocurrent on incident light quanta energy is well described by this relationship near the threshold. The linear part of this dependency is extrapolated to the $h\nu$ axis and the I_p value is determined as the photon energy at the interception point. I_p and A can also be estimated from electrochemical characteristics combined with UV absorption measurements. From the cyclic voltammetry curve of an organic compound showing oxidation peaks and taking −4.8 eV as the HOMO level for the ferrocene/ferrocenium redox system as a reference,[8] a HOMO level in eV can be calculated. Using the value of the optical band gap (ΔE_{opt}), which can be estimated by the absorption spectrometry, a LUMO value can be estimated.[9,10]

Applications

Hole-transporting hydrazones are mostly used in electrophotographic photoreceptors. Electrophotography is a complex process involving at least five steps, as shown in Fig. 4.[1] In the first step, the surface of the photoconductor drum is uniformly charged by a corona discharge. The next step is exposure. Parts of the photoconductor are discharged by light reflected from an image. Thus the information is transferred into a latent, electrostatic image on the surface of the photoconductor. In the third step, electrostatically charged and pigmented polymer particles of the toner are brought into the vicinity of the oppositely charged latent image thus transforming it into a real image. The next step is transfer. The toner particles are transferred from the surface to a sheet of paper by giving the back side of the paper a charge opposite to the toner particles. In the last step, the image is permanently fixed by melting the toner particles to the paper between two heated rollers. The electrophotographic drum is then cleaned of any residual toner and is ready for the next copy. Most modern organic photoreceptors have a dual-layer configuration. The main advantage of such a configuration is the possibility of separate optimisation of the two layers. The charge generation layer usually consists of a dye such as titanyl phthalocyanine dispersed in a polymer binder, *e.g.* poly(vinylbutyral). The charge transport layer is prepared by embedding an organic charge transport material into a polymer host, *e.g.* polycarbonate. A charge transport layer has to contain a large amount (up to 50% or even more) of the active compound to ensure effective transport of charges. Introduction of such a large amount of low-molar-mass charge transport compound into the polymer host can lead to crystallization. To prevent this problem, charge transporting compounds which do not readily crystallize are preferable.

Organic charge-transporting materials are also widely used in the photoreceptors of laser printers.[11] The electrophotographic process taking place in the printers is almost the same as in photocopiers except for direct generation of the image by a laser instead of the optical system in a copier. Photoreceptors of laser printers have to absorb in the long wavelength region of the spectrum.

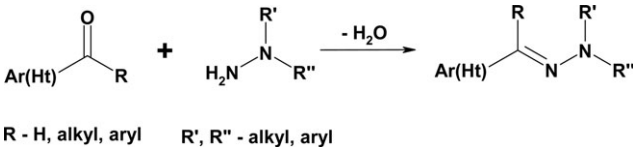

R - H, alkyl, aryl R', R'' - alkyl, aryl

Scheme 1

Low-molar-mass hydrazones

The synthetic route to charge-transporting hydrazones usually includes formylation of an aromatic or heteroaromatic compound followed by condensation of the obtained aldehyde with mono or disubstituted hydrazine (Scheme 1). This is a relatively simple synthesis. It does not require any expensive chemicals or catalysts. Toluene, water, various alcohols, such as methanol or ethanol, or ethers, such as tetrahydrofuran, dioxane or diethyl ether, can be used as solvents for such reactions. Hydrazone formation can be catalyzed by adding several drops of acid or using salts, *e.g.* sodium acetate.[12]

The wide range of heterocyclic/aromatic aldehydes and mono/disubstituted hydrazines allows tailoring not only of charge transport properties, but also of thermal and optical properties of the hydrazones. The morphological stability is an important issue for the amorphous charge transport materials, which are used either alone as film-forming materials or embedded in inert polymer hosts (molecularly doped polymers). Molecularly doped polymers containing small hydrazone molecules often tend to crystallize and the morphological stability of amorphous electroactive layers prepared from such materials is often not sufficient. Low-molar-mass hydrazones capable of existing in a solid amorphous state are superior in this case.

The suitable absorption pattern for the hydrazones can be achieved using appropriate starting compounds for their synthesis. Electrons of the aryl groups (R′, R″ in Scheme 1) are conjugated through the lone pair electrons of the nitrogen atoms; therefore the absorption of the hydrazones is extended compared with that of the starting compounds. The basic properties of aromatic hydrazones are their facile oxidizability and the ability to transport positive charges *via* the radical cation species. The ability to form electrically a stable radical cation that can undergo an infinite number of redox cycles is the major requirement for organic semiconductors.

Various electrophores have been used in the design and synthesis of low-molar-mass hydrazones. Derivatives with the basic skeleton of aminophenylhydrazone and different substituents at the nitrogen atom were widely used as the components of molecularly doped polymers to study charge carrier transport phenomena in these systems. The synthesis of such compounds is usually started from the preparation of an appropriate aminobenzaldehyde and followed by the reaction of the prepared aldehydes with differently substituted hydrazines. Kitamura and Yokoyama[13] made an attempt to find a correlation between the chemical structure and hole drift mobility of such hydrazones. They observed charge mobility variation over *ca.* two orders of magnitude by systematic changes in the substituents at the nitrogen atoms of the hydrazone moieties. The differences in hole mobilities were discussed in terms of the concepts of polyfunctionality and intramolecular mobility. From molecular structure considerations and molecular orbital calculations, the importance of the positive charge distribution on a molecule in the cation radical was emphasized for the molecular design of high-mobility charge-transporting compounds.

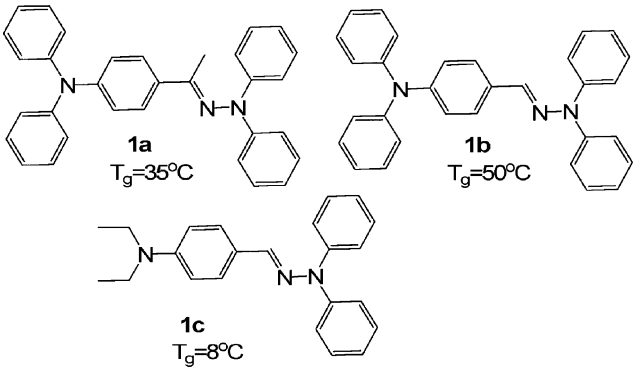

Fig. 5 Hydrazones based on aromatic amines.

Shirota *et al.*[14] has synthesized and studied aromatic amine-based hydrazones, the structures of which are shown in Fig. 5.

All the compounds shown in Fig. 5 form transparent amorphous films by solution casting as well as on cooling from the melt. Glass transition temperature (T_g) values of 35 °C, 50 °C and 8 °C were observed for **1a**, **1b** and **1c**, respectively. The glasses of **1a** and **1c** were found to be rather unstable. The compounds crystallize upon heating above T_g. However, the glass of **1b** was more stable. No crystallization upon heating above T_g was observed. Hole drift mobilities in amorphous films of the hydrazones shown in Fig. 5 and in host polymers molecularly doped with compounds **1a**–**1b** were studied by the time of flight method.[15] The values obtained are given in Table 1. Hole drift mobilities (μ_h) of 50 wt% solid solutions of **1a**–**1b** in polycarbonate (PC) were found to be more than one order of magnitude lower than those observed for the glasses of the net compounds. It is interesting to note that in the same conditions, the μ_h of arylaldehyde hydrazone **1b** is *ca.* twice as high as that of the corresponding aryl ketone hydrazone **1a**, in spite of the fact that there is no difference in the π-electron skeleton. The steric effect of the methyl-substituent in **1a** might affect the intersite distance and the intermolecular overlap of π-electrons. Charge transport properties of *p*-diethylaminobenzaldehyde *N*,*N*-diphenylhydrazone (**1c**) were studied in detail.[16,17] The charge transport in the supercooled liquid state of 4-diphenylaminobenzaldehyde methylphenylhydrazone (T_g = 30 °C) and **1b** was studied and compared with that in their molecular glasses.[18] Hole drift mobility in the supercooled liquid state in the temperature region above T_g was found to be lower than that predicted from the temperature dependence of the hole drift mobility of the glass in the region below T_g. The electric-field and temperature dependencies of the hole drift mobility were analyzed in terms of the disorder formalism.

Fujii *et al.*[19] have studied charge transport properties of the hydrazones shown in Fig. 6. Hole drift mobilities of solid solutions of **2a**–**2c** in bisphenol A polycarbonate (PC-A) (1 : 1) are given in Table 1. Hole mobilities in these

Table 1 Hole drift mobilities in amorphous layers of low-molar-mass hydrazones and in their solid solutions in polycarbonate

Charge transport material	μ/cm^2 V^{-1} s^{-1}	Electric field E/V cm^{-1}	Ref.
1a	7.0×10^{-5}	2.0×10^5	14,15
1a (50% in PC)	2.6×10^{-6}	2.0×10^5	14,15
1b	2.2×10^{-4}	2.0×10^5	14,15
1b (50% in PC)	8.7×10^{-6}	2.0×10^5	14,15
1c (47% in PC)	2.3×10^{-6}	2.0×10^5	20
2a (44% in PC-A)	8.5×10^{-6}	3.1×10^5	19
3c (47% in PC-A)	1.5×10^{-6}	2.0×10^5	20
3e (47% in PC-A)	3×10^{-7}	2.0×10^5	20
3f (47% in PC-A)	7.7×10^{-7}	2.0×10^5	20
4b	2.0×10^{-5}	2.0×10^5	22
4b (50% in PC-Z)	2.1×10^{-6}	2.0×10^5	22
4i	8.0×10^{-4}	2.0×10^5	22
4f	4.4×10^{-6}	3.0×10^5	22
4l (50% in PC-Z)	5.0×10^{-5}	2.0×10^5	22
4n	1.0×10^{-3}	2.0×10^5	22
4n (50% in PC-Z)	3.0×10^{-5}	2.0×10^5	22
6c	3.5×10^{-6}	2.0×10^5	28
6c (50% in PC-Z)	5.1×10^{-7}	2.0×10^5	28
6f	6.0×10^{-6}	2.0×10^5	28
6f (50% in PC-Z)	4.5×10^{-7}	2.0×10^5	28
7b	1.8×10^{-7}	2.0×10^5	29
8d	5.0×10^{-5}	2.0×10^5	30
8d (50% in PC-Z)	4.0×10^{-6}	2.0×10^5	30
8f (50% in PC-Z)	1.0×10^{-7}	2.0×10^5	30

molecularly-doped polymers increase with increasing polarizabilities and decrease with increasing dipole moments of the dopants. There is no information on the glass-forming abilities of hydrazones **2a**–**2c**.

Hirao and Nishizawa[20] have studied the effect of the polarity of hydrazones shown in Fig. 7 on charge carrier drift mobilities and diffusion coefficients in molecularly doped polymers containing these hydrazones. The decrease in charge mobility was observed with increasing dipole moment of the hydrazone molecules.

Diphenylamine, triphenylamine, carbazole or phenothiazine are moieties which contain several active positions for the reaction with electrophiles. In such a way di- or even triformyl derivatives can be obtained under Vilsmeier conditions and di- or trihydrazones can be easily synthesized.

The synthesis and hole-transport properties of 9-alkylcarbazolyl-based hydrazones have been reported in detail.[21] Hole drift mobilities in the amorphous layers of these materials were found to be of the order of 10^{-6}–10^{-2} cm^2 V^{-1} s^{-1} at an electric field of 1.0×10^5 V cm^{-1} at room temperature. This is a higher value than those observed for non-conjugated polymers and molecularly-doped polymer systems.

Also series of 9-alkyl, 9-phenyl- and 9-alkoxyphenylcarbazolyl mono and dihydrazones were synthesized, and their thermal, optical, and charge transport properties were reported.[22,23] Their general formulae are given in Fig. 8. The 9-alkyl-, 9-phenyl- and 9-alkoxyphenylcarbazolylhydrazones were prepared mainly by two-step syntheses. The first step was the formylation of 9-substituted carbazoles by a Vilsmeier method to get mono- and diformyl compounds. The second step was condensation of the synthesized aldehydes with differently substituted hydrazines.

9-Alkylcarbazole-based hydrazones with methyl substituents at the hydrazine N atom appeared to be more inclined to crystallization then diphenyl substituted hydrazones. 9-Phenyl- and 9-alkoxyphenylcarbazole-based hydrazones

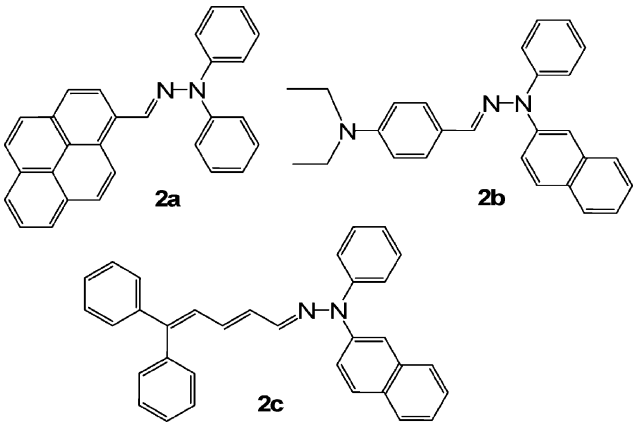

Fig. 6 Hydrazones based on aromatic amines.

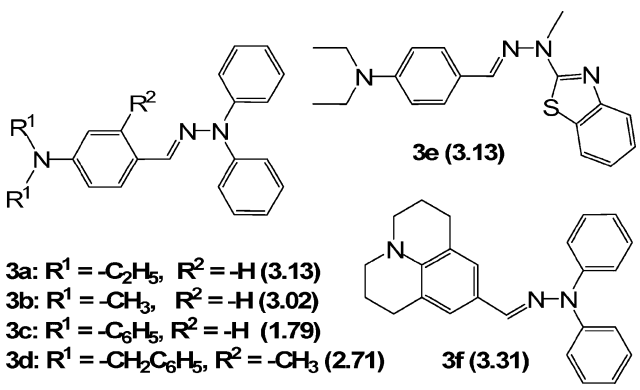

Fig. 7 Structures of hydrazones and the values of their permanent dipole moment in debye.

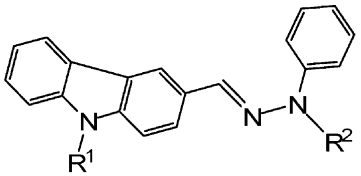

	4a	4b	4c	4d	4e	4f	4g	4h
R^1	Et	Ph	Ph	$PhOCH_3$	$PhOCH_3$	CH_3	$CH(CH_3)_2$	EtHex
R^2	Ph	CH_3	Ph	Ph	CH_3	Ph	Ph	Ph

EtHex : 2-Ethylhexyl

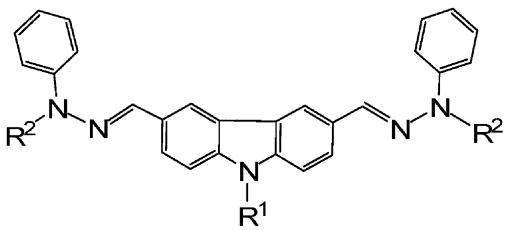

	4i	4j	4k	4l	4m	4n	4o	4p
R^1	Et	Hex	Ph	Et	Hex	Ph	$PhOCH_3$	$PhOCH_3$
R^2	CH_3	CH_3	CH_3	Ph	Ph	Ph	Ph	CH_3

Fig. 8 9-Alkyl-, 9-alkoxyphenyl and 9-phenylcarbazole-based hydrazones.

showed better glass-forming properties than 9-alkylcarbazole-based hydrazones. Compounds **4d**–**4h**, **4k**, **4n**, **4o** as well as **4p** form glasses. Apparently, the incorporation into the molecules of the rigid phenyl, alkoxyphenyl or branched alkyl groups, which hinder the packing of molecules, increases their ability to form glasses. The incorporation of the rigid phenyl group also increases the T_g of the glasses. Monohydrazones **4a**–**4e** showed lower T_g than the corresponding dihydrazones. Hydrazone **4h** was used as a photoconductive plasticizer in photorefractive systems because of its excellent transparency and fluidity.[24] The T_g of **4h** is 22 °C. The diphenyl substituted hydrazones showed better charge transport properties than their methylphenyl-substituted counterparts. The highest hole drift mobilities were observed in the amorphous films of **4l**, **4m** and **4n**.

The concentration dependence in the activation energy for charge transport in 9-ethylcarbazole-3-carbaldehyde diphenylhydrazone (**4a**) dispersed in polycarbonate was studied by Nomura and Shirota.[25] The activation energy gradually decreased with increasing **4a** concentration in the region of relatively low concentrations, but became nearly constant (0.4 eV) in the region of relatively high concentrations of **4a**. This behaviour contrasted with that observed for the 4-diphenylaminobenzaldehyde diphenylhydrazone (**1b**) containing system. The authors claimed that specific intermolecular interactions between molecules of **4a**, which have planar carbazole moieties, at relatively high concentrations might be responsible for such concentration dependence in the activation energy.

Morphological stability of molecular glasses can be improved by increasing the size of molecules. These concepts were demonstrated and described earlier by Shirota.[26] Increase in the size of molecule often also leads to enlargement of the system of conjugated π-electrons, which allows enhancement of charge carrier mobilities. Such a strategy was used in the design and synthesis of the 3,3′-dicarbazolyl-based hydrazones shown in Scheme 2.[27] These hydrazones form glasses and their amorphous films could be prepared on substrates by casting from solutions. T_g was in the range of 99–133 °C. The ionization potentials of hydrazones **5** measured by the electron photoemission technique ranged from 5.21 to 5.4 eV. Hole drift mobilities of 3,3′-dicarbazolyl-based hydrazones approached 10^{-5} cm^2 V^{-1} s^{-1} at an electric field of 3.2×10^5 V cm^{-1} at 25 °C.

Formyl derivatives of phenothiazine have also appeared to be useful in the synthesis of charge transporting hydrazones.[28] The structures of phenothiazine-based mono and dihydrazones are shown in Fig. 9. The synthesis was similar to that described for carbazolyl-based hydrazones. Phenothiazine-based hydrazones **6a**–**6f** can be transformed into the amorphous state. The T_g of the synthesized hydrazones strongly depends on the chemical structure of the molecule and range from 23 °C to 79 °C. Dihydrazones exhibit higher T_g than the core monohydrazones.

Dihydrazone **6f** showed better charge transport properties than monohydrazones **6a** and **6c**. The solid solutions of the hydrazones in bisphenol Z polycarbonate (PC-Z) exhibited hole drift mobilities one or two orders of magnitude lower than amorphous films of the pure compounds (*cf.* the data in Table 1). Comparison of charge transport properties of phenothiazine-based hydrazones **6** with those of carbazole-based hydrazones **4** reveals the superiority of the latter ones. The

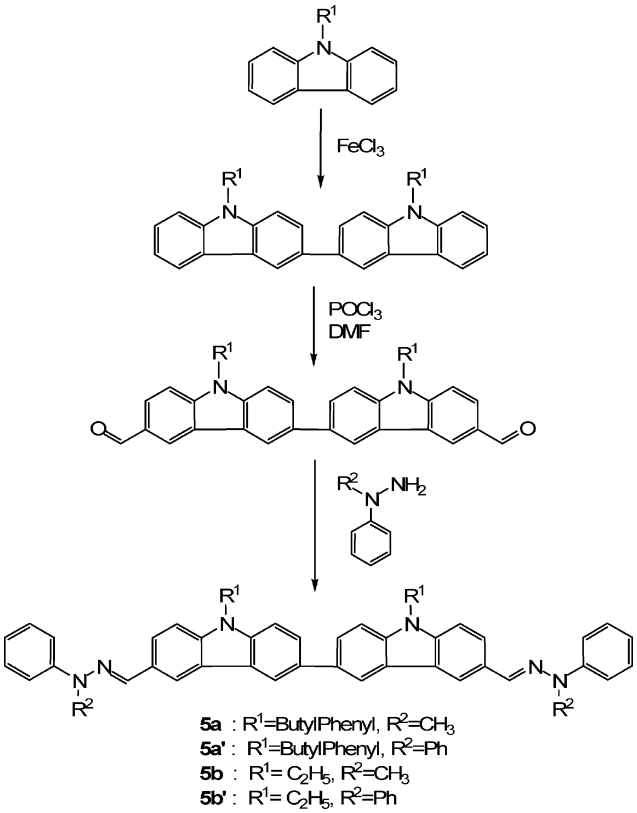

Scheme 2

values for the hole drift mobilities of carbazole-based hydrazones is one order of magnitude higher.

Hole-transporting hydrazones containing 3,4-ethylenedioxythiophene (EDOT) moieties were reported recently.[29] EDOT-based hydrazones were synthesized by a two-step synthetic route, as shown in Scheme 3. The hydrazone with phenyl substituents (**7a**) forms molecular glass, showing glass transition at 37 °C, contrary to **7b**, which shows no ability to form glass. The I_p value of hydrazone **7b**, with a methyl phenyl-substituted N atom of the hydrazine moiety, was found to be 5.6 eV and that of the diphenyl-substituted hydrazone **7a** was 0.15 eV lower. Hole drift mobility of 1.8×10^{-7} cm^2 V^{-1} s^{-1} was observed for the amorphous layer of **7b** at an electric field of 2×10^5 V cm^{-1} at 293 K.

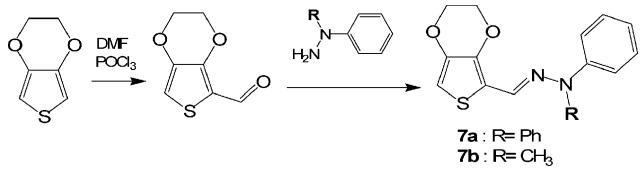

Scheme 3

Twin molecules such as 9-[2-(9*H*-carbazol-9-yl)cyclobutyl]-9*H*-carbazole and 9-[6-(9*H*-carbazol-9-yl)hexyl]-9*H*-carbazole and the corresponding derivative of phenothiazine have also been used in the synthesis of hole-transporting hydrazones.[30] The general formula of such hydrazones is shown in Fig. 10. Twin hydrazones were synthesized by a synthetic route similar to that described above. The starting twin compounds, prepared either by alkylation of carbazole or phenothiazine with dibromohexane or by cyclodimerization of 9*H*-vinylcarbazole, were transformed to the corresponding formyl derivatives by the method of Vilsmeier, and were then condensed with *N*,*N*-diphenylhydrazine or *N*-methyl-*N*-phenylhydrazine.

All hydrazone twin compounds shown in Fig. 10 form glasses. The T_g of hydrazones **8a**, **8b** (118 and 136 °C, respectively) containing rigid cyclobutane moieties are markedly higher than those of compounds **8c**, **8d** (81 and 91 °C, respectively) in which the carbazolyl moieties are linked by a flexible hexamethylene bridge. Phenothiazinyl-based hydrazone twin compounds **8e** and **8f** were obtained as amorphous substances with T_g of 79 and 91 °C, respectively. The T_g of the carbazole and phenothiazine-based compounds (**8c**–**8d**, and **8e**–**8d**) that have similar skeletons are comparable to each other. The values of the hole drift mobilities of the above described hydrazones in the form of glasses and of the solid solutions in host polymers are presented Table 1.

A series of carbazolyl-containing hydrazone molecules in which two identical bulky groups are linked by different aliphatic or aromatic linking units was reported.[31] This type of molecular structure allows a broad range of modifications by changing the length, flexibility and shape of the central link. The synthetic route to these derivatives involves the reaction of suitable aldehydes with phenylhydrazine, followed by the reaction with dibromoalkane or dibromoxylene (Scheme 4, Table 2). This is a convenient route for the preparation of hydrazone-twins under mild conditions and in high yields.

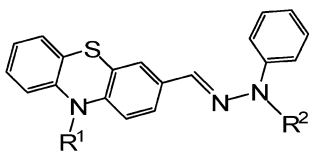

	6a	6b	6c
R^1	Et	Et	EtHex
R^2	Ph	CH_3	Ph

EtHex : 2-Ethylhexyl

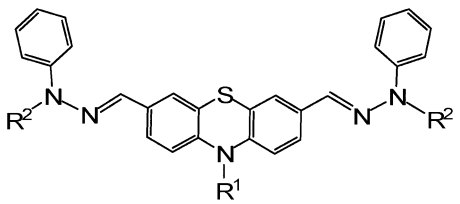

	6d	6e	6f
R^1	Et	Et	EtHex
R^2	Ph	CH_3	Ph

Fig. 9 10-Alkyl- and 10-phenylphenothiazinyl-based hydrazones.

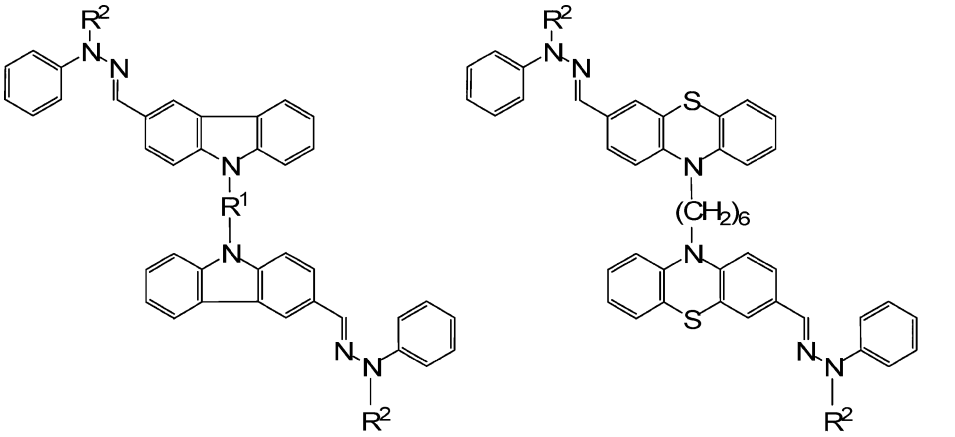

	8a	8b	8c	8d
R^1	Cb	Cb	Hex	Hex
R^2	CH_3	Ph	CH_3	Ph

Cb – cyclobutyl, Hex – hexyl

	8e	8f
R^2	CH_3	Ph

Fig. 10 The structures of hydrazone twin compounds.

The T_g of compounds **9a**–**9i** can be varied in a relatively wide range by changing the length of the linking fragment X and the aliphatic substituent R (Table 2). An increase in the aliphatic chain length R from ethyl to heptyl results in a decrease in T_g from 84 °C to 45 °C. An increase in the chain length of the linking bridge X from trimethylene to octamethylene leads to a decrease in T_g from 84 °C to 46 °C. The values for time-of-flight hole mobilities of solid solutions of twin hydrazones in PC-Z are presented in Table 2. The best hole transport properties were observed for the twin compounds **9b** and **9c** with the highest content of electrophores.

Hydrazone twin molecules possessing triphenylamino moieties, shown in Fig. 11, have also been reported.[31]

The ionization potential values for the amorphous films of hydrazone twin compounds **10a**–**10e** and charge mobility data for their 50% solid solutions in PC-Z are given in Table 3.

A series of hydrazone twin compounds (**11a**–**11f**) with different sulfur-containing linking fragments were prepared by synthetic routes involving the reaction of the heterocyclic or aromatic formyl derivatives with phenylhydrazine, followed by reaction with epichlorohydrin.[32] The last step was the reaction of the obtained epoxy derivatives with different aromatic/aliphatic dithiols. The general formula of these hydrazone twin compounds is shown in Fig. 12.

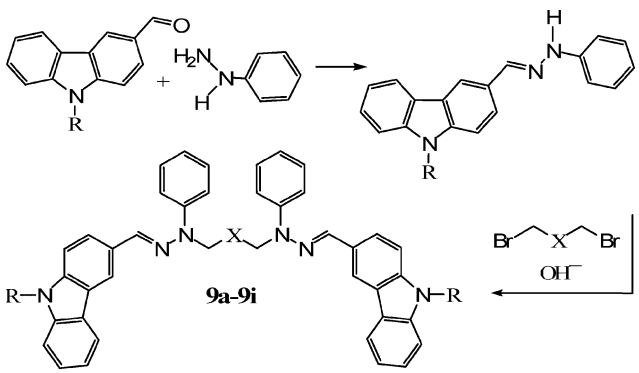

Scheme 4

Such molecular structure makes crystallization of these compounds difficult and facilitates glass formation. T_g of the sulfur-containing twin hydrazones shown in Fig. 12 range from 45 °C to 79 °C. The nature of the linking fragment Q and the structure of the electrophores (R) have a significant influence on the melting and glass transition temperatures of the compounds. These temperatures are lower for the twin compounds with triphenylamino (TPA) electrophores as compared with those containing 9-ethylcarbazolyl (EtCz) groups.

Hydrazone twin compounds with oxygen-containing linking bridges (Fig. 13) were synthesized in a similar way to sulfur-containing twin hydrazones except for the last stage in which the epoxypropyl substituted hydrazones were treated with the different dihydroxybenzenes.[33] The melting point of *para*-substituted derivative (**12**, Q = b, R = EtCz) is over 200 °C and the material is polymorphic; however it shows glass transition at 89 °C. The melting enthalpy of this compound is high and it is insoluble in most of the common organic solvents, except highly polar solvents such as dimethylformamide. On the other hand, the compound with an *ortho*-substituted benzene ring (**12**, Q = c, R = EtCz) was found to exist only in an amorphous state, and its glass transition temperature is lower than that of the compound with a *para*-substituted benzene ring.

These facts indicate the significance of the molecular symmetry in the glass formation of molecular materials. The presence of hydroxyl groups also influences the morphology of molecular materials.[33] This statement can be illustrated by the behavior under heating of the twin hydrazones **13a** and **13b** shown in Fig. 14.

Table 2 Glass transition temperatures and photoelectric characteristics of twin hydrazones **9a**–**9i**

Charge transport material	Structure of twin hydrazone		T_g/°C	I_p/eV	μ^a/cm^2 V^{-1} s^{-1}
	R	X			
9a	C_2H_5	$(CH_2)_8$	46	—	—
9b (40% in PC-Z)	C_2H_5	$(CH_2)_3$	84	5.44	1.1×10^{-5}
9c (40% in PC-Z)	C_2H_5	$(CH_2)_2$	79	5.34	1.7×10^{-5}
9d (40% in PC-Z)	$CH_3(CH_2)_6$	$(CH_2)_8$	29	—	—
9e (40% in PC-Z)	$CH_3(CH_2)_6$	$(CH_2)_3$	45	5.38	6.5×10^{-6}
9f (40% in PC-Z)	$C_6H_5(CH_2)_3$	$(CH_2)_3$	57	5.23	3.6×10^{-6}
9g (40% in PC-Z)	$CH_3(CH_2)_3$	$(CH_2)_3$	—	5.40	5.6×10^{-6}
9i (50% in PC-Z)	C_2H_5	*m*-C_6H_4	—	5.35	2.9×10^{-6}

[a] At an electric field of 6.4×10^{-5} V cm^{-1}.

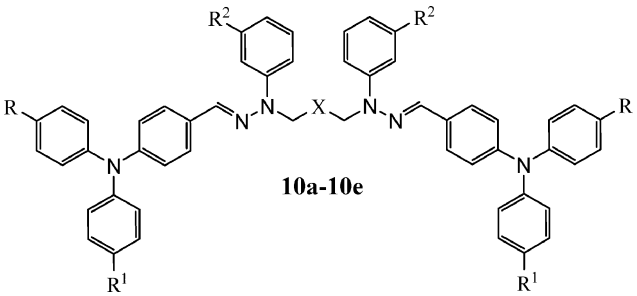

Fig. 11 General formula of hydrazone twin molecules with triphenylamino moieties.

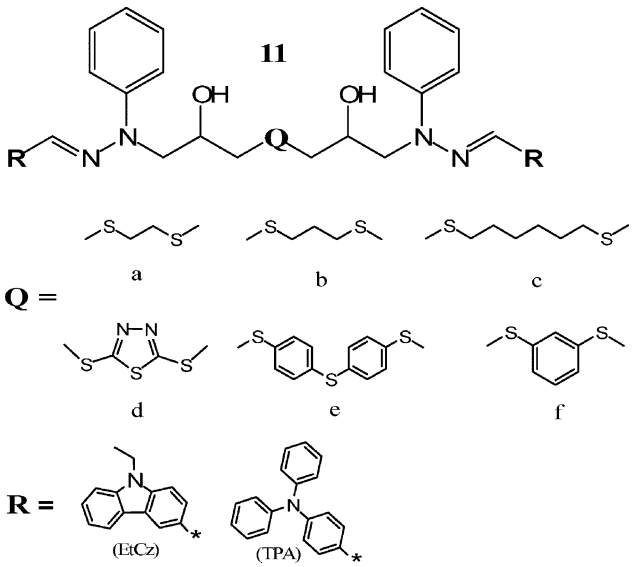

Fig. 12 The general formula of hydrazone twin compounds with sulfur-containing linking bridges.

Compound **13a**, containing no hydroxyl groups, was found to exist only in the amorphous state, while compound **13b**, containing these groups, can exist both in the crystalline and in the amorphous state. The T_g of compound **13a** (64 °C), which contains no hydroxyl groups, is considerably lower compared to that of **13b** (80 °C). These observations can be explained by the presence of hydrogen bonding sites in **13b**. The values for time-of-flight hole mobilities of the amorphous films of the selected twin hydrazones with sulfur- and oxygen-containing linking bridges and of their molecular mixtures with polymer host poly(vinyl butyral) (PVB) are presented in Table 4. The highest hole mobility values were observed for the materials containing a triphenylamine (TPA) moiety. The other important factor influencing charge transport properties is the origin of the substituents in hydrazone molecules. The hole mobility value for **13b**, which contains highly polar hydroxyl groups, is more than one order of magnitude lower than for **13a** which contains no hydroxyl groups.

Hydrazones possessing 1-phenyl-1,2,3,4-tetrahydroquinoline moieties have appeared to be effective hole transport materials for electrophotographic photoreceptors. The negatively charged dual layered photoreceptors with various squarylium dyes as charge generation materials and 1-phenyl-1,2,3,4-tetrahydroquinoline-6-carboxaldehyde *N*,*N*-diphenylhydrazone (**14**) (Fig. 15) as the hole transport material exhibited high photosensitivity for white light.[34]

Hydrazone **14** is a crystalline material that is not capable of forming amorphous films and it was used as a molecular dispersion in PC. The drift mobility of holes at a zero electric field limit in 50 wt% of **14** doped PC was found to be 8.6×10^{-7} cm^2 V^{-1} s^{-1} at 298 K.[35]

Table 3 Structures and photoelectric characteristics of twin hydrazones **10a**–**10e**

Charge transport material	Structure of twin hydrazone				μ_0/cm^2 V^{-1} s^{-1}	μ^a/cm^2 V^{-1} s^{-1}	I_p/eV
	R	R^1	R^2	X			
10a	CH_3	CH_3	H	*m*-C_6H_4	1.5×10^{-6}	4.0×10^{-5}	5.28
10b	H	H	CH_3	*m*-C_6H_4	2.4×10^{-6}	4.0×10^{-5}	5.41
10c	CH_3	H	H	*m*-C_6H_4	8.0×10^{-7}	2.2×10^{-5}	5.35
10d	CH_3	H	H	*p*-C_6H_4	4.0×10^{-7}	2.0×10^{-5}	5.33
10e	CH_3	H	H	*o*-C_6H_4	2.3×10^{-6}	3.3×10^{-5}	5.33

[a] At an electric field of 6.4×10^{-5} V cm^{-1} for the 50% solid solution in PC-Z.

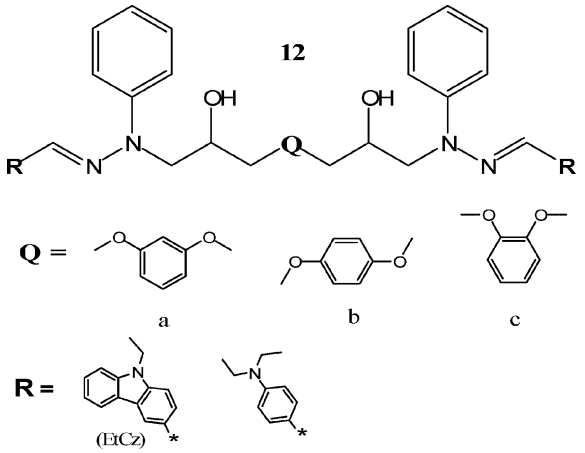

Fig. 13 The general formula of hydrazone twin compounds with oxygen-containing linking fragments.

Epoxy functionalized 1-phenyl-1,2,3,4-tetrahydroquinoline-based hydrazones **15** and **16** were synthesized starting from diphenylamine[36] as shown in Scheme 5.

The hole drift mobilities in solid solutions in PC-Z of these hydrazones exceeded 10^{-6} cm^2 V^{-1} s^{-1} at an electric field of 10^6 V cm^{-1}.[36] Epoxy functionalized hydrazones **15** and **16** were used in the synthesis of twin molecules possessing 1-phenyl-1,2,3,4-tetrahydroquinoline-based hydrazone moieties[37] (Scheme 6).

Twin compounds **17**–**20** were prepared by the reaction of 4,4′-thiobisbenzenethiol and 4,4′-dimercaptobiphenyl with 2 equivalents of the corresponding epoxy functionalized hydrazones **15** or **16** in the presence of a catalytic amount of triethylamine (TEA).[37] Twin compounds **17**–**20** were isolated as amorphous materials. X-Ray diffraction patterns of these compounds showed only broad halos, and DSC thermograms exhibited only glass transitions. Time-of-flight hole drift mobility data for the amorphous films of twin compounds **17**–**20** and for their 50% solid solutions in PC-Z are presented in Table 5. The highest hole mobilities, exceeding 10^{-5} cm^2 V^{-1} s^{-1} at an electric field of 6.4×10^5 V cm^{-1}, were observed for the amorphous films of compounds **17** and **19** which contain the *N*,*N*-diphenyl hydrazone unit. Twin compounds **18** and **20**, containing *N*-methyl-*N*-phenyl hydrazone units, exhibit slightly lower hole mobilities. This observation is explained by the slightly larger conjugated π-electron systems in **17** and **19**. The central linking fragment has practically no effect on the charge transport properties of the twin hydrazones. Hole mobilities in the solid solutions of 1-phenyl-1,2,3,4-tetrahydroquinoline-based hydrazones in PC-Z were found to be *ca*. one order of magnitude lower.

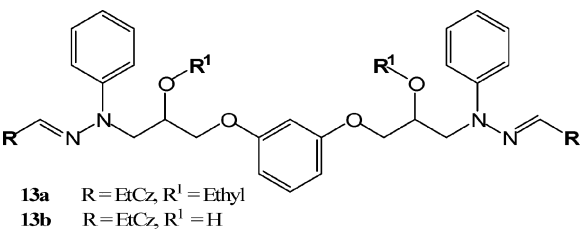

Fig. 14 The general formula of hydrazone twin compounds **13a** and **13b**.

Table 4 Hole drift mobilities of selected twin hydrazones with sulfur- and oxygen-containing linking bridges in the form of neat amorphous films and molecular mixtures with PVB

Charge transport material	X	R	μ^a/cm^2 V^{-1} s^{-1}
11	a	EtCz	3.5×10^{-5}
11 (50% in PVB)	a	EtCz	1.2×10^{-6}
11	a	TPA	1.0×10^{-4}
11 (50% in PC-Z)	a	TPA	7.3×10^{-6}
11	e	EtCz	1.3×10^{-5}
11	e	TPA	2.6×10^{-4}
13a	—	EtCz	1.0×10^{-4}
13b	—	EtCz	5.8×10^{-6}

[a] At an electric field of 6.4×10^5 V cm^{-1}.

Twin compounds possessing 4-(diethylamino)salicylaldehyde *N*,*N*-diphenylhydrazone moieties can also be used in electrophotography as hole-transporting materials.[38] The synthetic route to compounds **21**–**24** which have two 4-(diethylamino)salicylaldehyde *N*,*N*-diphenylhydrazone moieties is shown in Scheme 7.

The first step was the alkylation of 4-(diethylamino)salicylaldehyde *N*,*N*-diphenylhydrazone by epichlorohydrin to get the corresponding glycidyl ether. Twin hydrazone **21** was obtained by nucleophilic oxirane ring opening of the glycidyl ether with the starting hydrazone which possesses a hydroxyl group. Compound **22** was obtained by the reaction of the glycidyl ether with 4,4′-thiobisbenzenethiol. Twin molecules **23** and **24** were synthesized by the interaction of 4-(diethylamino)salicylaldehyde *N*,*N*-diphenylhydrazone with neopentyl glycol diglycidyl ether and 1,4-butanediol diglycidyl ether, respectively, at 70–75 °C in the presence of TEA. The ionization potential and charge mobility values for 4-(diethylamino)salicylaldehyde *N*,*N*-diphenylhydrazone-based twin compounds are given in Table 6. The best charge transport properties were observed for compound **21** which has the highest content of electrophores and the lowest number of polar hydroxyl groups.

Aromatic hydrazones are usually used in electrophotographic photoreceptors as molecular dispersions in inert polymer hosts. To enhance the hole-transporting ability, new material systems that allow a decrease in the concentration of the inactive polymer components and thus provide a higher concentration of hydrazone moieties are required. Star-shaped low molar mass or star-shaped dendritic molecular architectures are considered to be useful for this purpose. Dendritic

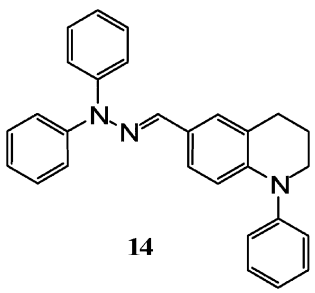

Fig. 15 Structure of 1-phenyl-1,2,3,4-tetrahydroquinoline-6-carboxaldehyde *N*,*N*-diphenylhydrazone (**14**).

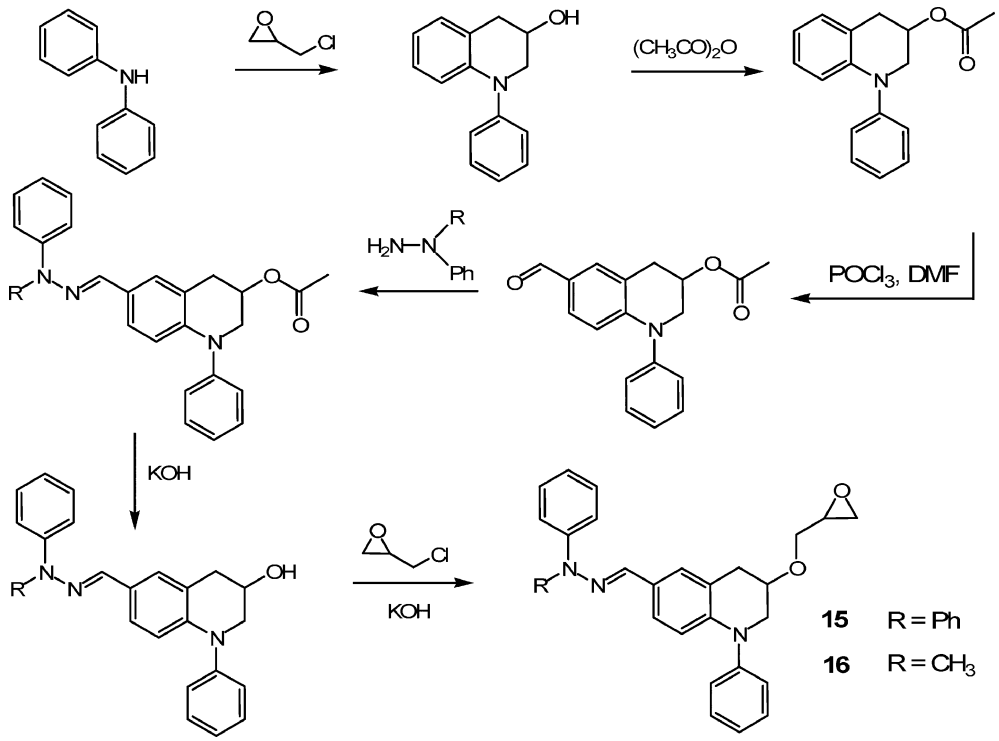

Scheme 5

star-shaped structures exhibit a more stable amorphous nature due to the geometry of these molecules, which does not favor close packing. The triphenylamine-based trihydrazones shown in Scheme 8 were synthesized by condensation of tris(*p*-formylphenyl)amine with *N*-methyl-*N*-phenyl hydrazine, *N*,*N*-diphenylhydrazine, *N*-1-naphthyl-*N*-phenylhydrazine, or *N*-2-naphthyl-*N*-phenylhydrazine.[39] Tris(*p*-formylphenyl)-amine, synthesized through Vilsmeier formylation of triphenylamine, reacted with these different hydrazines yielding 80, 77, 60, or 58% of the corresponding hydrazone. The hydrazines were obtained by the nitrosation and reduction reactions of the corresponding amines.

Hydrazones **26a** and **26b** were obtained as crystalline compounds and showed clear endothermic melting peaks in the first DSC heating scans at 247 and 241 °C, respectively. They formed glasses after cooling from the melt. Upon the second

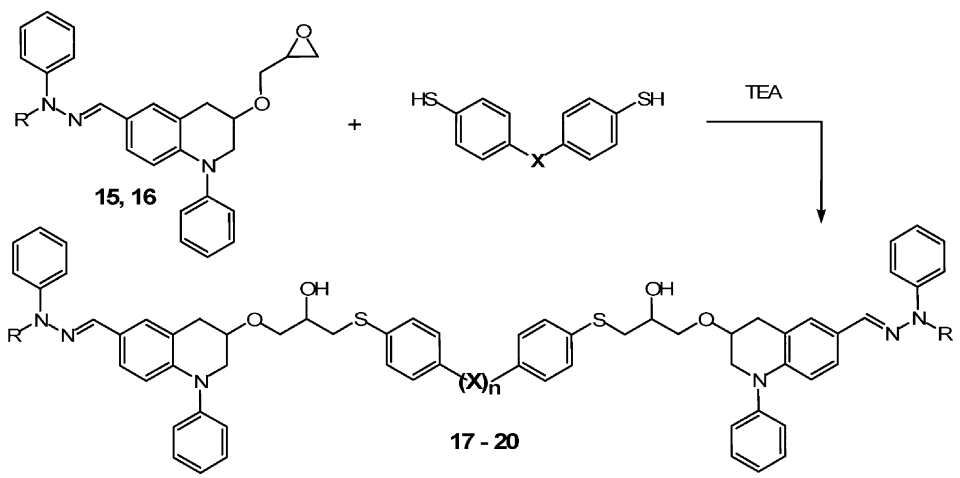

	15	16	17	18	19	20
R	Ph	CH_3	Ph	CH_3	Ph	CH_3
X	--	--	S	S	--	--
n	--	--	1	1	0	0

Scheme 6

Table 5 Hole mobility data for the amorphous films of **14**–**20** and for their 50% solid solutions in PC-Z

Charge transport material	μ_0/cm^2 V^{-1} s^{-1}	μ^a/cm^2 V^{-1} s^{-1}
14	8.6×10^{-7}	—
15 (50% in PC-Z)	10^{-7}	4.4×10^{-6}
16 (50% in PC-Z)	6.0×10^{-8}	4.6×10^{-6}
17	1.8×10^{-7}	1.8×10^{-5}
17 (50% in PC-Z)	1.8×10^{-8}	7.0×10^{-7}
18	6.0×10^{-8}	5.3×10^{-6}
18 (50% in PC-Z)	9.0×10^{-9}	2.0×10^{-7}
19	2.0×10^{-7}	1.3×10^{-5}
19 (50% in PC-Z)	1.7×10^{-8}	6.6×10^{-7}
20	1.0×10^{-7}	5.0×10^{-6}
20 (50% in PC-Z)	1.6×10^{-8}	5.3×10^{-7}

[a] At an electric field of 6.4×10^5 V cm^{-1}.

heating, they showed glass transitions at 74 and 81 °C, respectively. No crystallization was observed even when they were heated above T_g. Compounds **26c** and **26d** were obtained as amorphous materials and in DSC experiments showed only glass transitions at 86 and 87 °C, respectively. The stable amorphous films of **26c** and **26d** could be formed directly by solution coating due to the large substituents, which can hinder the regular arrangement and motion of the molecules and lead to formalization of the amorphous state.

Dendrimer **27d** was prepared in a multi-step synthesis as shown in Scheme 9.[40] First, the active hydrogen atom was blocked using phthalic anhydride and then formylation under Vilsmeier conditions was performed. The next steps were condensation with *N*,*N*-diphenylhydrazine and hydrolysis of

Table 6 Ionization potential and charge mobility data for hydrazones **21**–**24**

Charge transport material	μ_0/cm^2 V^{-1} s^{-1}	μ^a/cm^2 V^{-1} s^{-1}	I_p/eV
21 (50% in PVB)	1.8×10^{-8}	1.1×10^{-6}	5.16
22 (50% in PVB)	3.2×10^{-9}	1.6×10^{-7}	5.28
23 (50% in PVB)	4.4×10^{-9}	2.4×10^{-7}	5.23
24 (50% in PVB)	6.7×10^{-9}	4.6×10^{-7}	5.22

[a] At an electric field of 6.4×10^5 V cm^{-1}.

the protecting group. Then tris(*p*-formylphenyl)amine was treated with hydrazine **27c** and hydrazone dendrimer **27d** was obtained in 16% yield. The T_g of dendrimer **27d** was found to be 164 °C. The films of dendrimer **27d** were reported to be clear, transparent, homogeneous, and mechanically tough. UV-visible absorption maximum was observed at 418 nm. Cut-off wavelength of this dendrimer was 487 nm corresponding to the HOMO to LUMO excitation energy of 2.5 eV.

Tris- and tetrakismercapto derivatives were used as linking precursors in the synthesis of hole-transporting star-shaped amorphous molecular materials.[41] The nucleophilic opening of the oxirane ring of 4-(diphenylamino)benzaldehyde *N*-2,3-epoxypropyl-*N*-phenylhydrazone by refluxing the oxirane with trimethylolpropane tris(2-mercaptoacetate) or trimethylolpropane tris(3-mercaptopropionate) in the presence of TEA gave compounds **28a** and **28b** (Scheme 10).

In the same manner the amorphous hole-transporting molecular material **29** shown in Fig. 16 which possesses four

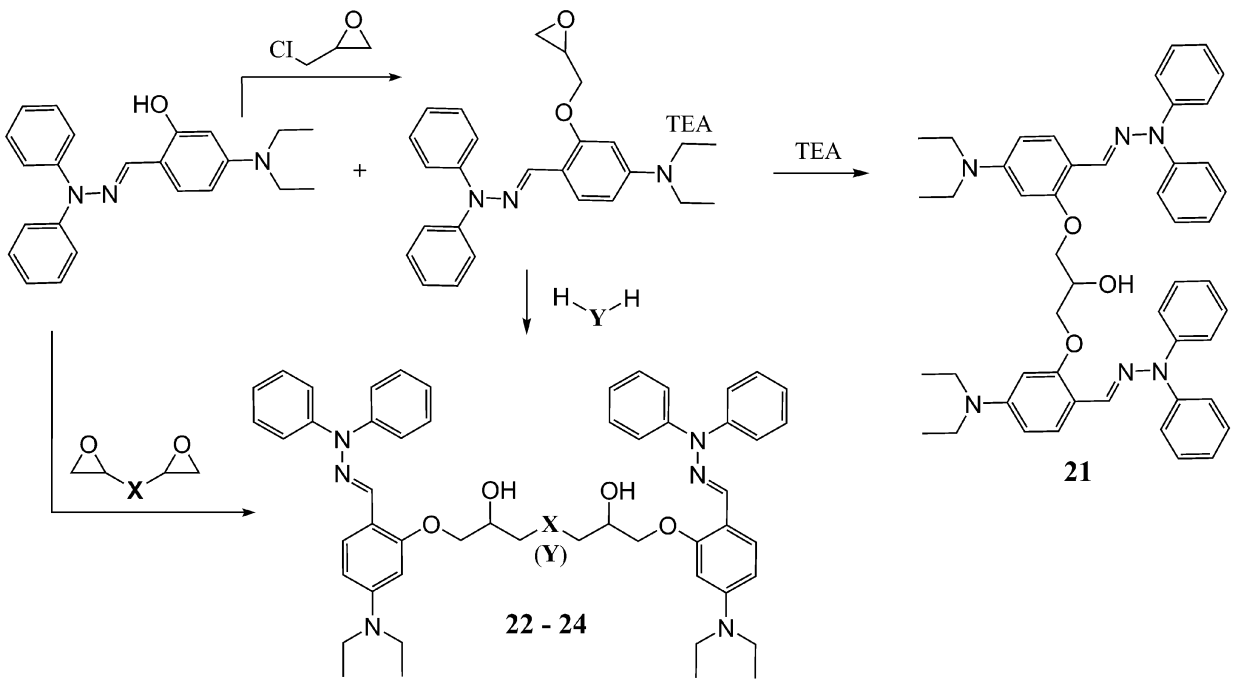

22 Y = —S—C$_6$H$_4$—S—C$_6$H$_4$—S— ; **24** X = $CH_2O(CH_2)_4OCH_2$.

23 X = $CH_2OCH_2C(CH_3)_2CH_2OCH_2$;

Scheme 7

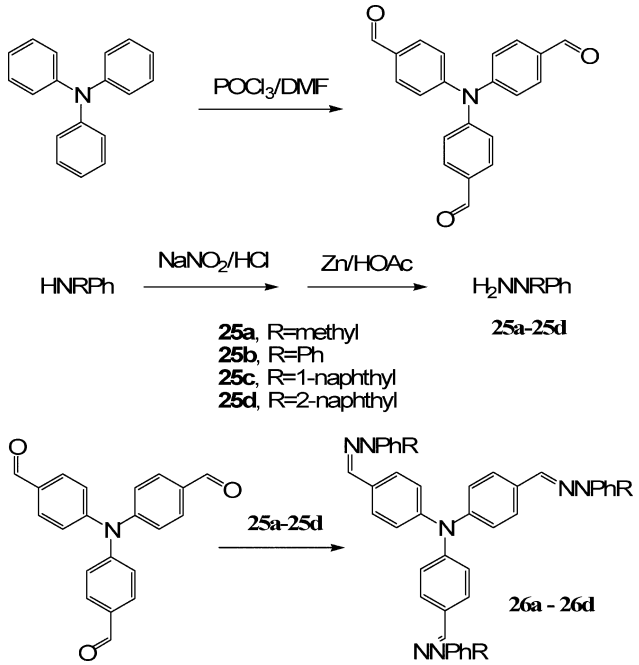

Scheme 8

hydrazone moieties was obtained in the reaction of penta erythritol tetrakis(2-mercaptoacetate) with 4-(diphenylamino)benzaldehyde *N*-2,3-epoxypropyl-*N*-phenylhydrazone.[41]

Branched hydrazones **28a**, **28b** and **29** are amorphous molecular materials with both ester and hydroxyl groups. They are compatible with the host polymers widely used in electrophotographic photoreceptors, *i.e.* with PC-Z and PVB. Table 7 lists the hole mobility data for molecularly doped polymers containing **28a**, **28b** and **29**.[41]

Pyrazolines as heterocyclic hydrazones are also within the scope of this review. Kitayama *et al.*[42] showed that 1,3,5-triaryl-2-pyrazolines form stable glasses at room temperature and even well above it. The authors compared hole mobilities in 1,3-diphenyl-5-(*p*-chlorophenyl)-2-pyrazoline, the structure of which is shown in Fig. 17, in the single crystalline state (mp 130 °C) and in the glassy state ($T_g = 16.5$ °C). The hole mobility in a single crystal was almost independent of the applied electric field, and was found to be *ca.* 10^{-2} cm^2 V^{-1} s^{-1}. In the glassy state, the hole mobility dropped to 10^{-5} cm^2 V^{-1} s^{-1}.

Later pyrazoline derivatives with dimeric structures were synthesised in order to improve their ability to form stable amorphous films and were applied in organic electroluminescent devices as hole transport materials.[43] The synthetic path to one of the dimmers is given in Scheme 11. 1,3,5-Triaryl-2-pyrazolines are available by condensation of the appropriate arylhydrazine with an α,β-unsaturated ketone (chalcone) under acidic conditions.

The fluorescence of the molecule shown in Scheme 11 was blue in the solid state.

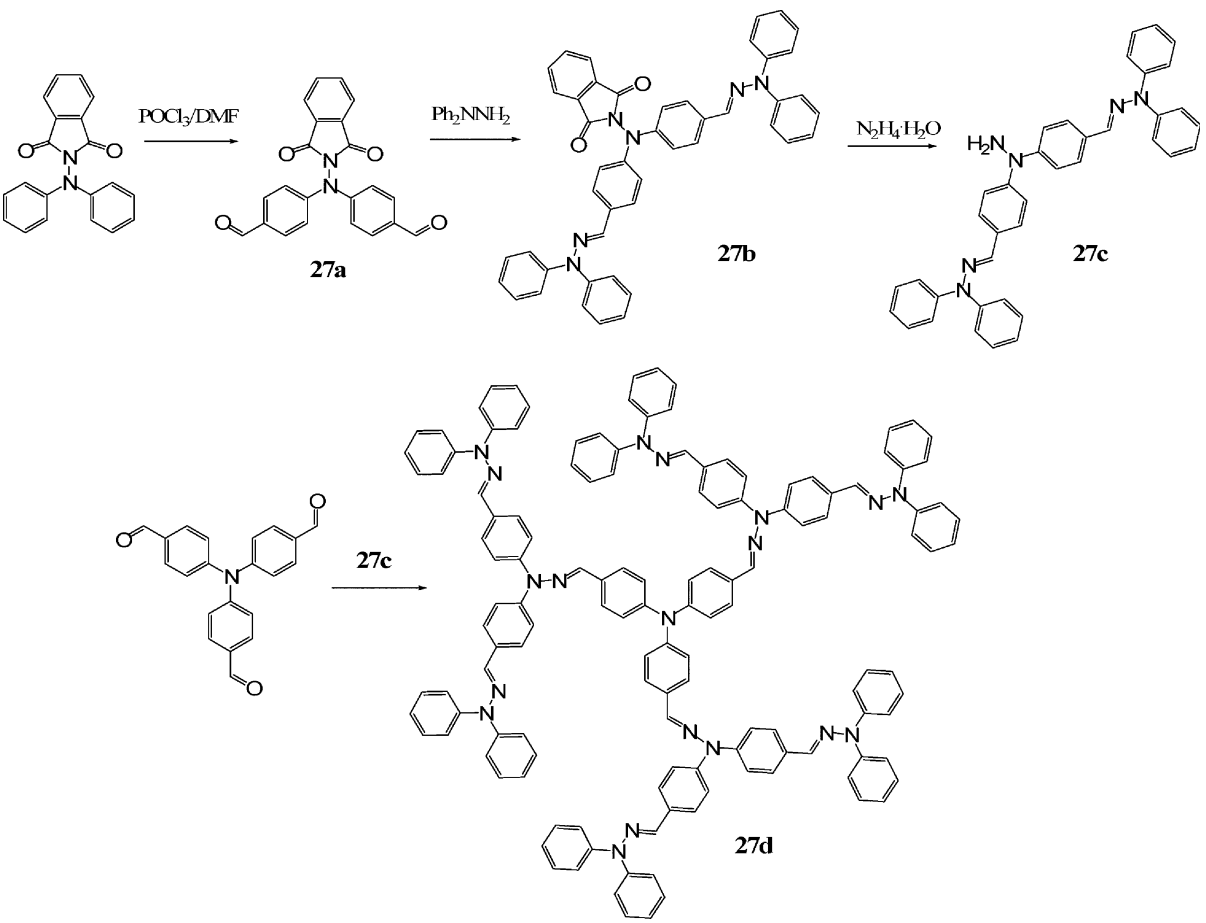

Scheme 9

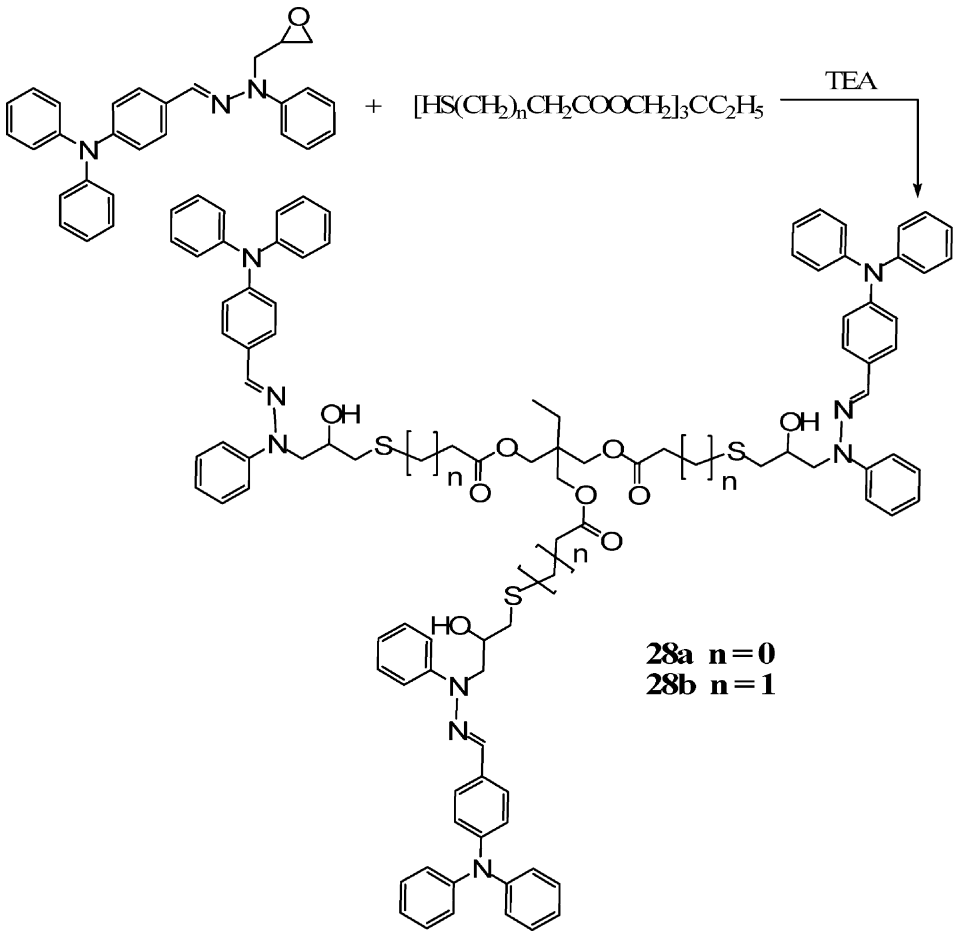

Scheme 10

Polymeric hydrazones

Polymeric hydrazones containing electrophores both in the main chain and as pendants have been reported. Polymer **30** (Fig. 18), which has side chain hydrazone moieties for non-linear optical applications, was synthesized by free radical copolymerization of 2-[3-(diphenylhydrazonomethyl)indol-1-yl]ethyl methacrylate with 2-[3-(6-nitrobenzoxazol-2-yl)indol-1-yl]ethyl methacrylate using a feed molar ratio of 1 : 1.[24] The polymer with a weight average molar mass M_w of 22 000 g mol^{-1} and T_g of 145 °C was obtained. It formed a stable

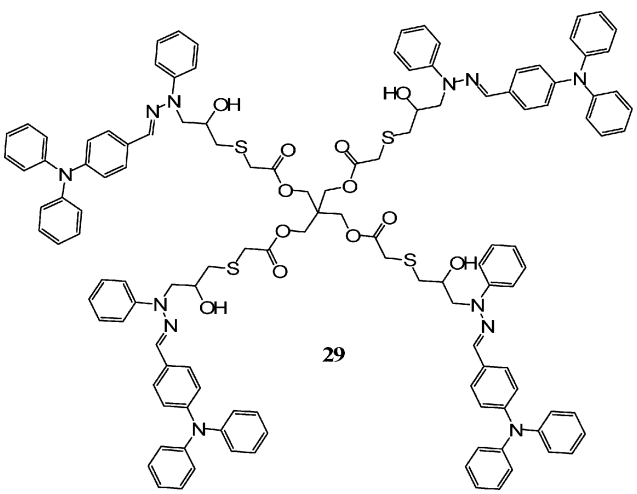

Fig. 16 Hole-transporting molecular material with four hydrazone moieties.

Table 7 Hole mobility data for 1 : 1 molecular dispersions of **28a**, **28b** and **29** in PC-Z and PVB

Charge transport material	μ_0/cm^2 V^{-1} s^{-1}	μ^a/cm^2 V^{-1} s^{-1}
28a (50% in PVB)	5.6×10^{-8}	1.4×10^{-6}
28a (50% in PC-Z)	9.0×10^{-7}	5.4×10^{-5}
28b (50% in PVB)	6.0×10^{-8}	1.0×10^{-6}
28b (50% in PC-Z)	8.0×10^{-7}	3.0×10^{-5}
29 (50% in PVB)	1.2×10^{-8}	7.7×10^{-7}
29 (50% in PC-Z)	1.0×10^{-7}	2.0×10^{-6}

[a] At an electric field of 6.4×10^5 V cm^{-1}.

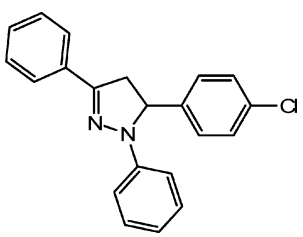

Fig. 17 Structure of 1,3-diphenyl-5-(*p*-chlorophenyl)-2-pyrazoline.

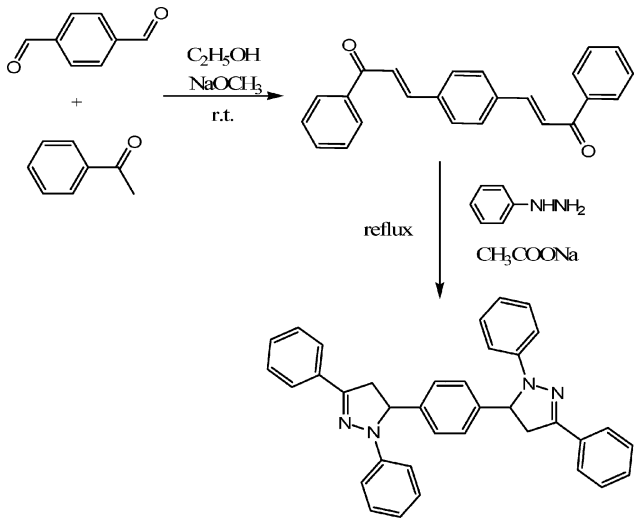

Scheme 11

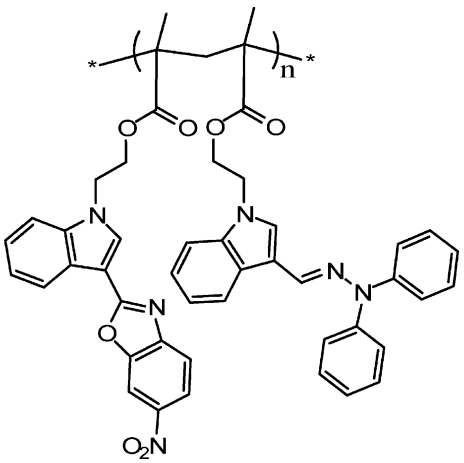

Fig. 18 Structure of polymer **30**.

amorphous film from THF solution. Photoconductivity of polymer **30** was directly proportional to the laser intensity and it increased as the applied electric field increased. The photoconductive sensitivities were 1.7×10^{-10} S cm W^{-1} and 5.0×10^{-10} S cm W^{-1} under 0.4 and 0.6 MV cm^{-1}, respectively.

D. W. Kim *et al.*[44] reported on a nonlinear optical side-chain copolymer containing a carbazolyldinitrophenylhydrazone moiety. It was prepared by copolymerization of methyl methacrylate and 6-[3-(2,4-dinitrophenylhydrazonomethyl)carbazol-9-yl]hexyl methacrylate (**31**, see Fig. 19) using a feed mole ratio of 3 : 1. The copolymer showed a glass transition at 138 °C, and an absorption maximum at 412 nm.

Poly(*N*-(2,3-epoxypropyl)carbazole) (PEPK) is a widely studied oligomeric photoconductor.[45] However, due to the high ionization potential, which reaches 5.86 eV,[46] this oligomer is not suitable for organic electrophotographic photoreceptors. A derivative of PEPK possessing hydrazone moieties was synthesized using a Vilsmeier formylation of PEPK,

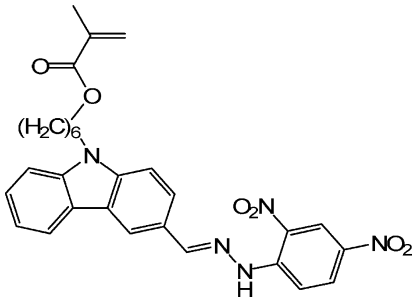

Fig. 19 Structure of 6-[3-(2,4-dinitrophenylhydrazonomethyl)carbazol-9-yl]hexyl methacrylate (**31**).

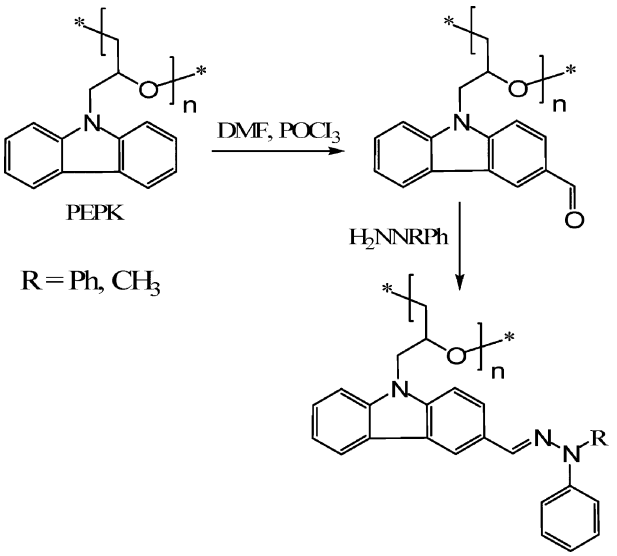

Scheme 12

followed by the reaction with *N*,*N*-diphenylhydrazine or *N*-methyl-*N*-phenylhydrazine (Scheme 12).[47]

Ionization potentials of the obtained oligomers containing *N*,*N*-diphenylhydrazone or *N*-methyl-*N*-phenyl hydrazone moieties were found to be 5.4 eV and 5.5 eV, respectively.

Fluorene copolymers containing the [aza(2,7-dibromofluorene-9-ylidene)methyl]diphenylamine (FDPA) moiety were designed and synthesized for organic light emitting diodes in order to improve the charge carrier balance of polyfluorene through exciton confinement.[48] The synthetic route to the fluorene-based random copolymers, poly(BEHF-*co*-FDPA)s, is shown in Scheme 13.

Poly[9,9-bis(2-ethylhexyl)fluorene-2,7-diyl] (PBEHF) and the random copolymers were synthesized through a Ni(0)-mediated polymerization known as the Yamamoto coupling reaction. The copolymer containing only 1% of FDPA, poly(99BEHF-*co*-1FDPA), exhibits a photoluminescence emission that is significantly red-shifted with respect to that of PBEHF. The copolymers exhibit luminescence maxima in the yellow region of the spectrum in the range from 530 to 540 nm, whereas the PBEHF film shows a fluorescence maximum in the deep blue region at 424 nm. The electroluminescent devices constructed using the copolymers exhibited better device performances than the device prepared from PBEHF.

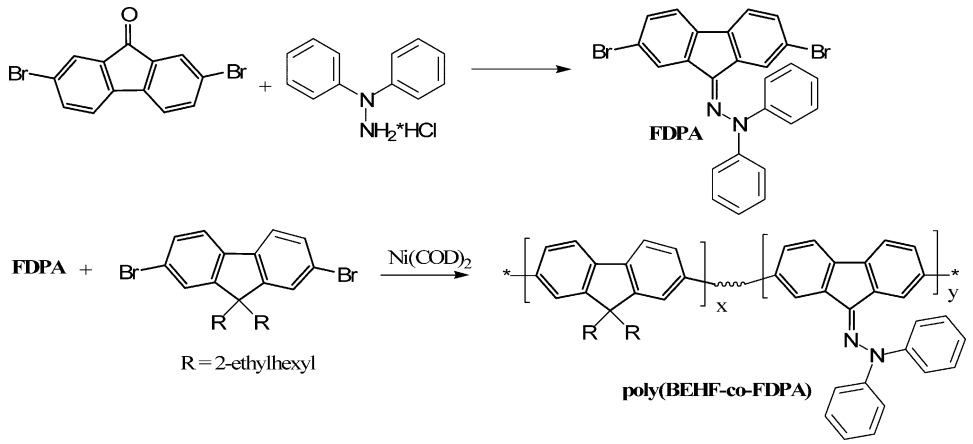

Scheme 13

This enhancement of performance is due to a more efficient charge carrier balance in the devices, which arises because of the effective exciton confinement (or charge carrier trapping) in FDPA groups.

Hole-transporting polymers containing hydrazone moieties in the main chain have also been synthesized.[49] The general formula of the polymers is shown in Scheme 14.

The first step in the synthesis of diepoxy monomer (Scheme 15) was Vilsmeier formylation of 9-ethylcarbazole, triphenylamine or 4-methyltriphenylamine. The second step was condensation of the diformyl compounds with phenylhydrazine to obtain dihydrazones. The monomers (diepoxides) were obtained by the interaction of the obtained dihydrazones with epichlorohydrin in the presence of KOH.

Polymers with number average molecular weights M_n ranging from 6700 to 9100 were obtained by copolyaddition of the monomers with 4,4′-thiobisbenzenethiol or 2,5-dimercapto-1,3,4-thiadiazole. The charge transporting chromophores appeared to have a significant influence on the T_g of the polymers. T_g was lower for the polymers with triphenylamine moieties as compared with those containing carbazolyl moieties. The lowest T_g was observed for the polymer containing the 4-methyltriphenylamine moiety. Hole drift mobilities in the amorphous films of the polymers exceeded 10^{-4} cm^2 V^{-1} s^{-1} at an electric field of 10^6 V cm^{-1}. These are rather high mobilities for amorphous non-conjugated polymeric charge transport materials. Hole mobilities in polymers containing triphenylamine moieties were *ca.* one

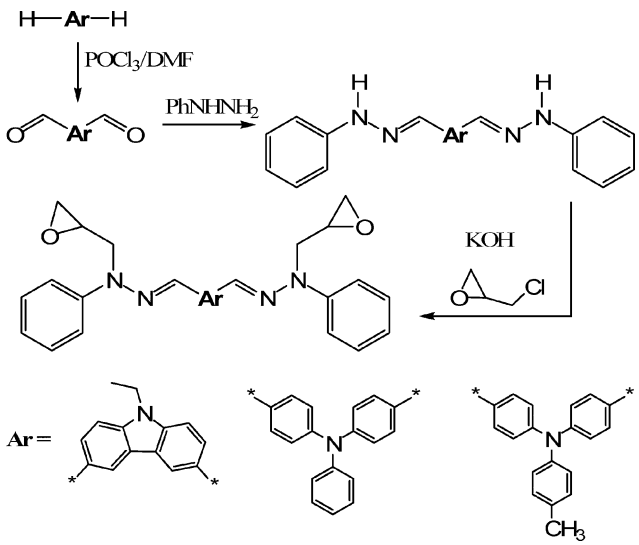

Scheme 15

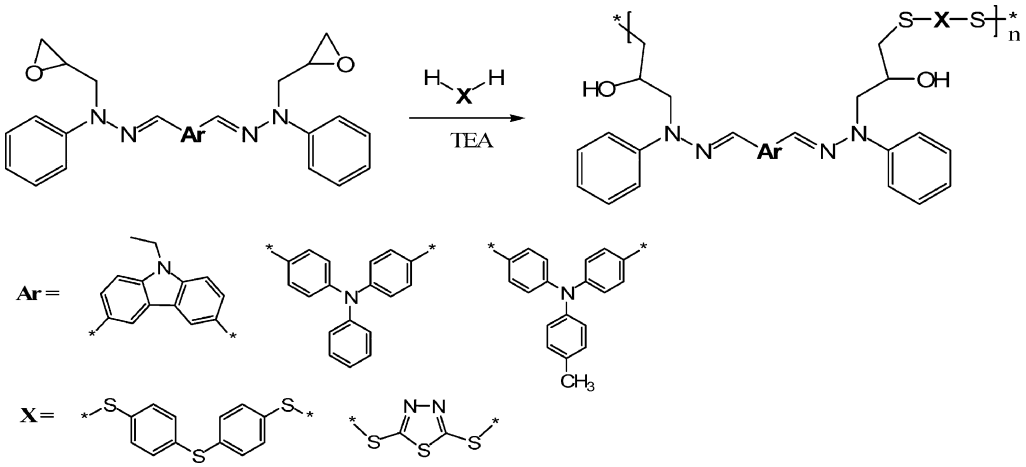

Scheme 14

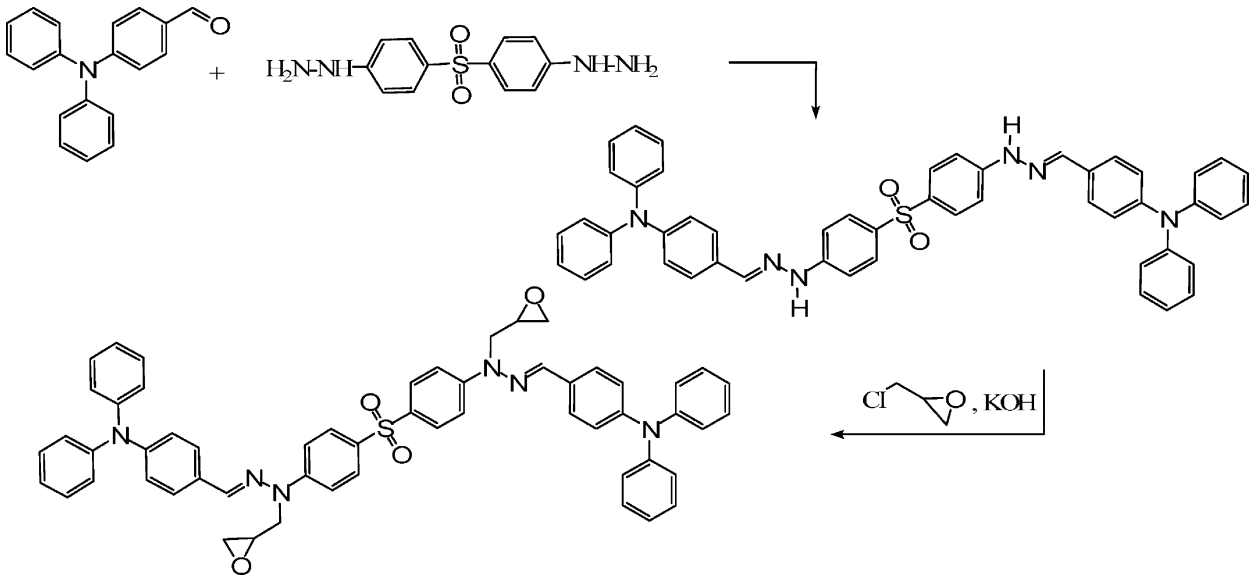

Scheme 16

order of magnitude higher than in polymers containing the carbazolyl group.

Bis(4-hydrazinophenyl)sulfone was also used for the synthesis of hydrazone main chain polymers.[50,51] Diepoxy monomers were synthesized as shown in Scheme 16.

The first step was the condensation of bis(4-hydrazinophenyl)sulfone with two equivalents of 4-(diphenylamino)benzaldehyde. The second step was the alkylation of the obtained intermediate dihydrazone with epichlorohydrin in the presence of KOH to get the diepoxy monomer. Polyaddition of the monomer with 4,4′-thiobisbenzenethiol or 2,5-dimercapto-1,3,4-thiadiazole in THF was carried out in the presence of TEA at the reflux temperature (Scheme 17). Hole drift mobilities in the amorphous films of these polymers exceeded 10^{-5} cm^2 V^{-1} s^{-1} at an electric field of 10^6 V cm^{-1}.

Polymeric hydrazones (**32** and **33** shown in Fig. 20) were prepared by polycondensation of bis(4-hydrazinophenyl)-sulfone with differently substituted diformyl carbazoles.[51] It was not possible to estimate the charge transport properties of these polymers due to their insufficient solubility. Hole drift mobilities in the amorphous films of the 50% solid solutions of

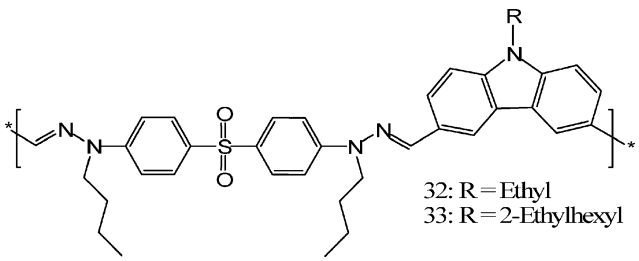

Fig. 20 Structure of polymers **32** and **33**.

the model compounds in PC-Z exceeded 10^{-5} cm^2 V^{-1} s^{-1} at high electric fields.

For some electrophotographic photoreceptors, such as that of the belt format on a flexible support, special requirements are raised with respect to the mechanical properties. They have to possess enhanced bending and stretching stability. In addition, charge transport layers of electrophotographic photoreceptors often have to be resistant to organic solvents. For these reasons, cross-linkable hydrazone-based charge transport materials were developed.[52] Cross-linkable charge

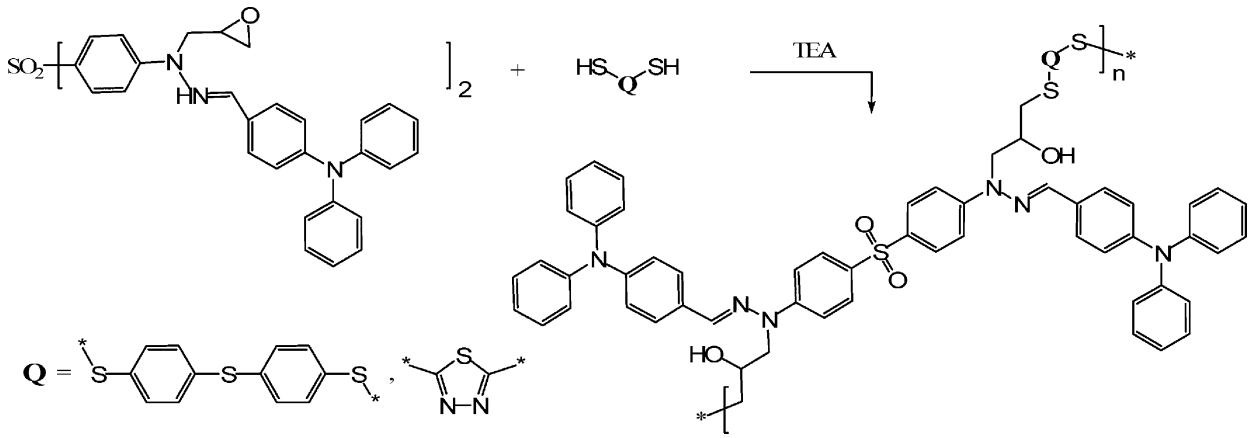

Scheme 17

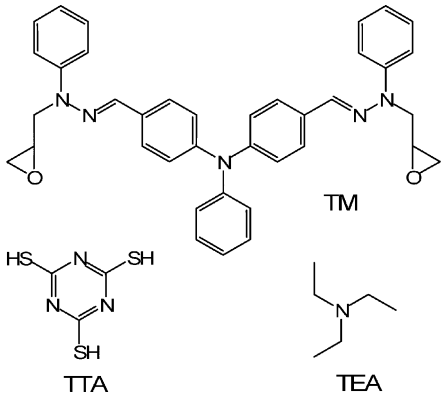

Fig. 21 Components for cross-linkable hole-transporting layers.

transport materials are useful in the preparation of multilayer solvent resistant electrophotographic photoreceptors. The components of one such cross-linkable composition are shown in Fig. 21.

Cross-linking of such a system takes place in *ca.* 1 h at 80 °C, and clear, insoluble layers are obtained without a significant decrease in charge carrier properties. Cross-linkable hydrazones with vinyloxyethyl groups have also been reported.[53]

From all the examples given above, it is evident that polymeric hydrazones are generally amorphous and they can form thin films on substrates. However their molecular weights remain low and mechanical properties are rather poor. In applications with strict requirements with respect to mechanical properties, cross-linkable hydrazones could be an efficient option.

Conclusions

During the past decades, many efforts have been made in the development of both low-molar-mass and polymeric hole-transporting hydrazones. The advantages of the hydrazones over other classes of organic semiconductors is their relatively simple and low cost synthesis and high charge carrier mobilities reaching 10^{-2} cm^2 V^{-1} s^{-1}. The wide range of heterocyclic/aromatic aldehydes and mono/disubstituted hydrazines allows tailoring of the charge transport, thermal and optical properties of the hydrazones. Among hole-transporting hydrazones, the large π-conjugated systems of triphenylamine–carbazole-based hydrazones allow high hole drift mobilities to be achieved. Hole mobilities of the hydrazones increase with decreasing dipole moments of the molecules. Hydrazone twin compounds have been widely synthesized and studied. Change in the linking groups allows variation of photoelectrical and thermal properties of such materials. The introduction of hydroxyl groups enables an increase in glass transition temperatures and improvement in the morphological stability of the glasses of twin hydrazones. Hydrazones with reactive functional groups represent a promising class of cross-linkable hole-transporting materials.

Acknowledgements

This work was supported by the Lithuanian Science and Studies Foundation and through a European social fund agency / Postdoctoral Fellowship of R.L. (grant no. ESF/2004/2.5.0-03-384/BPD-158/1).

References

1 P. M. Borsenberger and D. S. Weiss, in *Organic Photoreceptors for Imaging Systems*, Marcel Dekker, New York, 1998.
2 Y. Shirota and H. Kageyama, *Chem. Rev.*, 2007, **107**, 953–1010; M. Thellakat, *Macromol. Mater. Eng.*, 2002, **287**, 442–461.
3 W. D. Gill, *J. Appl. Phys.*, 1972, **43**, 5033.
4 H. Bässler, *Phys. Status Solidi B*, 1993, **175**, 15H. Bässler, in *Organic Molecular Solids; Properties and Applications*, CRC Press, Boca Raton, 1997, p. 267H. Bässler, *Polym. Adv. Technol.*, 1998, **9**, 402.
5 W. E. Spear, *Proc. Phys. Soc., London, Sect. B*, 1957, **B70**, 669–675; R. G. Kepler, *Phys. Rev.*, 1960, **119**, 1226–1229.
6 E. Montrimas, V. Gaidelis and A. Pažėra, *Liet. Fiz. Rinkinys*, 1966, **6**, 569–578; I. P. Batra, K. K. Kanazawa and H. Seki, *J. Appl. Phys.*, 1970, **41**, 3416–3422.
7 R. Lygaitis and V. Jankauskas, unpublished work.
8 J. Pommerehne, H. Vestweber, W. Guss, R. F. Mark, H. Bässler, M. Porsch and J. Daub, *Adv. Mater.*, 1995, **7**, 551–554.
9 R. Cernini, X.-C. Li, G. W. C. Spencer, A. B. Holmes, S. C. Moratti and R. H. Friend, *Synth. Met.*, 1997, **84**, 359–360.
10 H. Ishii, K. Sugiyama, E. Ito and K. Seki, *Adv. Mater.*, 1999, **11**, 605–625.
11 M. Lutz, *J. Imaging. Technol.*, 1985, **11**, 254A. Kukuta, in *Infrared Absorbing Dyes*, ed. M. Matsuoka, Plenum Press, New York, 1990, ch. 12.
12 Y. P. Kitaev and B. I. M. Buzykin, in *Hydrazony*, Nauka, Moskva, 1974, p. 21.
13 T. Kitamura and M. Yokoyama, *J. Appl. Phys.*, 1991, **69**, 821–826.
14 K. Nishimura, T. Kobota, H. Inada and Y. Shirota, *J. Mater. Chem.*, 1991, **1**, 897–898.
15 K. Nishimura, H. Inada, T. Kobota, Y. Matsui and Y. Shirota, *Mol. Cryst. Liq. Cryst.*, 1992, **216**, 503–510.
16 J. X. Mack, L. B. Schein and A. Peled, *Phys. Rev. B: Condens. Matter Mater. Phys.*, 1989, **39**, 7500–7508.
17 P. M. Borsenberger, L.-B. Lin and E. H. Magin, *Phys. Status Solidi B*, 1997, **204**, 721–728.
18 S. Nomura, K. Nishimura and Y. Shirota, *Mol. Cryst. Liq. Cryst.*, 1998, **313**, 247–252.
19 A. Fujii, T. Shoda, S. Aramaki and T. Murayama, *Jpn. J. Appl. Phys.*, 1997, **36**, 2739–2743; A. Fujii, T. Shoda, S. Aramaki and T. Murayamas, *J. Imaging Sci. Technol.*, 1999, **43**, 430–436.
20 A. Hirao and H. Nishizawa, *Phys. Rev. B: Condens. Matter Mater. Phys.*, 1997, **56**(6), R2904–R2907.
21 Y. Shirota, S. Nomura and H. Kasgeyama, *Proc. SPIE–Int. Soc. Opt. Eng.*, 1998, **3476**, 132–141.
22 Y. Sato, M. Yajima and H. Kanai, *Polym. Prepr. Jpn.*, 1991, **40**, 3588.
23 J. Ostrauskaite, V. Voska, V. Antulis, V. Gaidelis, V. Jankauskas and J. V. Grazulevicius, *J. Mater. Chem.*, 2002, **12**, 3469–3474; A. Matoliukstyte, R. Lygaitis, J. V. Grazulevicius, V. Gaidelis, V. Jankauskas, M. Montrimas, Z. Tokarski and N. Jubran, *Mol. Cryst. Liq. Cryst.*, 2005, **427**, 107–116.
24 J. Hwang, H. Moon, J. Seo, S. Y. Park, T. Aoyama, T. Wada and H. Sasabe, *Polymer*, 2001, **42**, 3023–3031.
25 S. Nomura and Y. Shirota, *Chem. Phys. Lett.*, 1997, **268**, 451–464.
26 Y. Shirota, *J. Mater. Chem.*, 2000, **10**, 1–25; Y. Shirota, *J. Mater. Chem.*, 2005, **15**, 75–93.
27 R. Lygaitis, J. V. Grazulevicius, V. Gaidelis, V. Jankauskas, J. Sidaravicius, Z. Tokarski and N. Jubran, *Mol. Cryst. Liq. Cryst.*, 2005, **427**, 95–106.
28 A. Danilevicius, J. Ostrauskaite, J. V. Grazulevicius, V. Gaidelis, V. Jankauskas, Z. Tokarski, N. Jubran, J. Sidaravicius, S. Grevys and A. Dzena, *J. Photochem. Photobiol., A*, 2004, **163**, 523–528.
29 R. Lygaitis, J. V. Grazulevicius, F. Tran Van, C. Chevrot, V. Jankauskas and D. Jankunaite, *J. Photochem. Photobiol., A*, 2006, **181**, 67–72.
30 J. Ostrauskaite, V. Voska, G. Buika, V. Gaidelis, V. Jankauskas, H. Janeczek, J. D. Sidaravicius and J. V. Grazulevicius, *Synth. Met.*, 2003, **138**, 457–461; J. Simokaitiene, A. Danilevicius, S.

Grigalevicius, J. V. Grazulevicius, V. Getautis and V. Jankauskas, *Synth. Met*., 2006, **156**, 926–931.
31 *US Pat*., 6 749 978, 2004.
32 V. Getautis, O. Paliulis, I. Paulauskaite, V. Gaidelis, V. Jankauskas, J. Sidaravicius, Z. Tokarski, K. Law and N. Jubran, *J. Imaging Sci. Technol*., 2004, **48**, 265–272J. Nusrallah, Z. Tokarski, R. Moudry, V. Getautis, T. Malinauskas, V. Gaidelis, V. Jankauskas and E. Montrimas, *IS&T's NIP20: International Conference on Digital Printing Technologies*, Salt Lake City, UT, 2004, pp. 552–556.
33 Z. Tokarski, N. Jubran, V. Getautis, O. Paliulis, M. Daskeviciene, I. Paulauskaite, V. Jankauskas, V. Gaidelis and J. Sidaravicius, *IS&T's NIP19: International Conference on Digital Printing Technologies*, New Orleans, LA, 2003, pp. 702–707.
34 S. H. Hwan, N. K. Kim, K. N. Koh and S. H. Kim, *Dyes Pigm*., 1998, **39**, 359–369.
35 Y. Kanemitsu, *Phys. Rev. B: Condens. Matter Mater. Phys*., 1992, **46**, 14182–14185.
36 V. Getautis, A. Stanisauskaite, T. Malinauskas, J. Stumbraite, V. Gaidelis and V. Jankauskas, *Monatsh. Chem*., 2006, **137**, 1401–1409.
37 V. Getautis, J. Stumbraite, V. Gaidelis, V. Jankauskas, V. Paulauskas and A. Kliuciu, *Synth. Met*., 2007, **157**, 35–40.
38 *US Pat*., 7 144 665, 2006; *US Pat*., 6 991 882, 2006.
39 K. J. Jiang, Y. L. Sun, K. F. Shao and L. M. Yang, *Chem. Lett*., 2004, **33**, 50–51.
40 H. Nam, D. H. Kang, J. K. Kim and S. Y. Park, *Chem. Lett*., 2000, **29**, 1298–1299.
41 *US Pat*., 7 118 840, 2006.
42 H. Kitayama, M. Yokoyama and H. Mikawa, *Mol. Cryst. Liq. Cryst*., 1981, **69**, 257.
43 T. Sano, T. Fujii, Y. Nishio, Y. Hamada, K. Shibata and K. Kuroki, *Jpn. J. Appl. Phys*., 1995, **34**, 3124–3127.
44 D. W. Kim, S. Y. Park and S. I. Hong, *Polym. J*., 1999, **31**, 55–60.
45 J. V. Grazulevicius, P. Strohriegl, J. Pielichowski and K. Pielichowski, *Prog. Polym. Sci*., 2003, **28**, 1297–1353.
46 S. Grigalevicius, G. Blazys, J. Ostrauskaite, J. V. Grazulevicius, V. Gaidelis and V. Jankauskas, *J. Photochem. Photobiol., A*, 2003, **154**, 161–167.
47 *US Pat. appl*., 20050221212, 2005.
48 D.-H. Hwang, M.-J. Park, J.-H. Lee, N.-S. Cho, H.-Ku Shim and Ch. Lee, *Synth. Met*., 2004, **146**, 145–150.
49 V. Getautis, J. V. Grazulevicius, T. Malinauskas, V. Jankauskas, Z. Tokarski and N. Jubran, *Chem. Lett*., 2004, **33**, 1336–1337; V. Getautis, J. V. Grazulevicius, M. Daskeviciene, T. Malinauskas, D. Jankunaite, V. Gaidelis, V. Jankauskas, J. Sidaravicius and Z. Tokarski, *Polymer*, 2005, **46**, 7918–7922; V. Getautis, J. V. Grazulevicius, M. Daskeviciene, T. Malinauskas, V. Gaidelis, V. Jankauskas and Z. Tokarski, *J. Photochem. Photobiol., A*, 2006, **180**, 23–27.
50 V. Getautis, J. V. Grazulevicius, M. Daskeviciene, T. Malinauskas, V. Jankauskas, J. Sidaravicius and A. Undzenas, *Eur. Polym. J*., 2007, **43**, 3597–3603.
51 E. Jasiukaityte, J. Ostrauskaite, J. V. Grazulevicius and V. Jankauskas, *J. Optoelectron. Adv. Mater*., 2006, **8**, 1323–1327.
52 V. Getautis, M. Daskeviciene, T. Malinauskas, V. Gaidelis, V. Jankauskas and Z. Tokarski, *Synth. Met*., 2005, **155**, 599–605.
53 R. Budreckiene, G. Buika, J. V. Grazulevicius, V. Jankauskas and Z. Tokarski, *Synth. Met*., 2007, **156**, 677–684; R. Budreckiene, G. Buika, J. V. Grazulevicius, V. Jankauskas and B. Staniskiene, *J. Photochem. Photobiol., A*, 2006, **181**, 257–262.

